Superexchange and lattice distortions in the spin--Peierls system CuGeO3

Geertsma, W.; Khomskii, D. I.

Published in:
ArXiv

Publication date:
2000

Superexchange and lattice distortions in the spin–Peierls system $CuGeO_3$.

Wiebe Geertsma[1,2)] and D. Khomskii[2)],

1) UFES-CCE/Depto de Fisica,

Fernando Ferrari s/n, Campus Goiabeiras,

29060–900 VITORIA–ES (Brasil);

2) Solid State Physics Laboratory,

Nijenborgh 4,

9747–AG GRONINGEN

(The Netherlands).

September 1, 2006

Abstract

We present a study of the nearest–neighbor (nn) and next–nearest–neighbor (nnn) exchange constants between magnetic Cu centers of the spin–Peierls material $CuGeO_3$. The dependence of these constants on the lattice parameters (modified e.g. by variation of temperature, pressure or doping) is calculated. Based on the observation that the bond angles are more susceptible than the bond lengths we propose the so–called "*accordion*" model for the description of the properties of $CuGeO_3$. We show that the *nn* exchange constant in the CuO_2 ribbon is very sensitive to the presence and position of the side group Ge with respect to this ribbon. The angle between the two basic units the CuO_2 ribbon and the GeO_3 zig–zag chain is, besides the Cu-O-Cu angle in the ribbon, one of the principal lattice parameters determining the *nn* exchange in the *c* direction. The microscopic calculations of different exchange constants and their dependence on the lattice parameters are carried out using different schemes (perturbation theory; exact diagonalization of Cu_2O_2 clusters; band approach). The results compare favorable with experiment. The influence of Si doping is also calculated, and

the reasons of why it is so efficient in suppressing the spin–Peierls phase are discussed. Thus the consistent microscopic picture of the properties of $CuGeO_3$ emerges.

PACS: 75.10, 75.30E, 75.30H.

(Submit to Phys. Rev. B)

Keywords:theory, exchange, magnetism, semiconductors, spin-Peierls Transition, linear chain.

Short title: spin–Peierls transition in $CuGeO_3$.

1 INTRODUCTION

The compound $CuGeO_3$ shows a spin–Peierls (SP) transition at 14 K: in each Cu chain the Cu cations dimerize and the spins form singlets. In this paper we study the exchange constants as a function of variations in the lattice parameters in the uniform spin phase as well as the SP phase. Changes in the lattice parameters can also be caused by applying pressure, or doping.

The plan of this paper is as follows. In the next subsections of this introduction we discuss the relevant structural, magnetic and magnetoelastic data. We finish this introduction with a general qualitative discussion of the theory of superexchange applied to this specific compound.

In the following sections we give a detailed account of the calculation of the exchange constants. First, in section 2 we give details of a fourth–order perturbation theory approach. We show that the usually neglected side groups (in the case of $CuGeO_3$ this is Ge) have in this particular case a large influence on the sign and magnitude of the nearest–neighbor (nn) exchange interaction. The influence of this Ge side group is studied.

Using perturbation theory we calculate the nn (sections 2.1 and 2.2) and next–nearest–neighbor (nnn) exchange (section 2.3) constants in the c (chain) direction as well as in the a and b direction. The values of the exchange constants thus obtained are quite reasonable, but their dependence on the lattice parameters strongly deviates from the experimental results. Therefore, in section 3 we use a different method, calculating the states of a Cu_2O_2 plaquette exact. This method gives quite satisfactory results for the lattice parameter (e.g. pressure and temperature) dependence of these exchange constants.

In order to account for multiple spin transfer paths we also performed a calculation using a band model for the anion states. The results reported in section 4 of the latter compare well with those obtained from the exact diagonalization of the Cu_2O_2 plaquette in section 3. Finally, in section 6 we give a discussion of the results; the conclusions and summary can be found in the final section 7.

1.1 The structure.

Before we discuss the magnetic properties it is convenient to describe relevant structural details. The structure of $CuGeO_3$ in the high temperature (HT) phase and in the SP phase has been determined by Braden et al [1]. Some results of their analysis can be found in table 1. In fig. 1 we have indicated the principal structural parameters important for our discussion of the exchange constants in the c direction. In the HT phase all Cu and all Ge ions are equivalent. The Cu have a near ideal square–planar coordination by O2 and these edge–sharing squares form a CuO_2 ribbon in the c direction. There are two O1 ions at a distance 2.755 $\mathring{A}$ nearly perpendicular to the ribbon, which would complete a tetragonally distorted octahedral coordination of Cu. This distance is too large to be of importance for the local electronic structure of Cu. The Ge have a nearly ideal tetrahedral coordination of O: two O2, shared with two CuO_2 ribbons, and two O1's. The $\angle$ O–Ge–O angles are about 109^0, very near to the ideal tetrahedral angle. The interatomic distance of the two O2 neighbors of a Ge is: 2.82 $\mathring{A}$. These two O2 connect two Cu in different ribbons along the b–axis. This is illustrated in fig. 2

Our preferred description of this system is as follows: linear GeO_3 chains of corner sharing GeO_4 tetrahedra, and CuO_2 ribbons of edge sharing CuO_4 squares, both units in the c direction. These two units share the O – which we will call the *hinges* of the structure – of the CuO_2 ribbon: at each side of the CuO_2 ribbon one GeO_3 chain, which form a *neutral undulating two dimensional layered* structure in the b direction (see fig. 5.

The interatomic distance of O2–O2, which connect two Cu in different ribbons along the a–axis, illustrated in fig. 3, is 3.06 $\mathring{A}$. This is much longer than twice the usually used ionic radius of O^{2-} for 6–fold coordination, which is about 1.40 ± 0.05 $\mathring{A}$, but nearly equal to twice the van der Waals radius of oxygen (2×1.52 $\mathring{A}$). This signifies that the bonding between two layers as defined in the preceding paragraph is small, and probably of the van der Waals type. A much smaller ionic radius of O^{2-} of about 1.25 $\mathring{A}$, fits the interatomic distances: Ge–O2 and Cu–O2 and the O2–O2 forming the bridge between two Cu in the same ribbon. This small ionic radius for O agrees with the rule from structural chemistry that a decrease in the coordination number causes a decrease in the ionic radius: in our

case O2 is coordinated by only three cations.

Other important structural factors for the calculation of the superexchange interactions are the *bond angles*. The most important angle is *bridge* angle $\phi = \angle$Cu–O–Cu in the ribbon plane, which is slightly larger than 90^0. The deviation of this angle from 90^0, β, determines the sign of the *nn* superexchange. Another important angle is the *hinge* angle $\alpha = \angle(\mathrm{O_2}\text{–}\mathrm{O_2})_{\mathrm{bridge}}$–Ge, which is about 160^0. These angles change as a function of pressure, doping, temperature and at the SP transition. In the SP phase the hinge and bridge angle have two distinct values (see table 1) due to the dimerization of the Cu chains. A very simplified model for this SP transition is presented in fig. 4. It is predominantly these angular variations which determine the properties of $CuGeO_3$.

The angles which determine the transfer in the a and b direction are given in fig. 3 and 2: the angles $\rho_a = \angle(\mathrm{O2}\text{–}\mathrm{O2})_{\mathrm{bridge}}$ –O_a and $\rho_b = \angle(\mathrm{O2}\text{–}\mathrm{O2})_{\mathrm{bridge}}$–$\mathrm{O}_b$, which are about 120^0 and $\theta_a = \angle(\mathrm{O2}\text{–}\mathrm{O2})_{\mathrm{a}}$–Cu and $\theta_b = \angle(\mathrm{O2}\text{–}\mathrm{O2})_{\mathrm{b}}$–Cu, which are about 110^0. These angles show only very small changes as a function of temperature and through the SP transition.

1.2 The magnetic properties.

The magnetic properties – as well as properties related to it – of $CuGeO_3$ in the ordered SP phase can well be described by the Cross–Fisher [2, 3] theory, however magnetic properties above the SP transition in the uniform phase do not agree with the usual 1D–Heisenberg spin 1/2 model with *nn* exchange J_{nn} only. Also a consistent interpretation of these properties based on this model seems impossible because it leads to widely different values for this exchange constant.

In table 2 we have collected experimental values for the exchange constants of $CuGeO_3$. The exchange constants in the c direction are defined by the Heisenberg Hamiltonian:

$$H_H = J_{nn} \sum_i (1 + \delta(T)(-1)^i) S_i S_{i+1} + J_{nnn} \sum_i S_i S_{i+2}. \tag{1.1}$$

Some authors do not specify how they define their exchange constants, which can easily lead to confusion. At present a model which includes also *nnn* exchange J_{nnn} along the Cu chain, gives the most consistent set of exchange parameters. Assuming $J_{nn} \approx 11$ to

15 meV and the frustration parameter $\gamma = J_{nnn}\ /J_{nn} \approx .24$ – .51 an agreement can be obtained between model calculation and experiments: high temperature (HT) susceptibility, magnetic specific heat, magnon dispersion. We consider the exchange constants determined in [15] as the most reliable set. For the exchange constants in the a and b direction we rely on the ones determined by Nishi et al [6]. These are rather small, compared with the interactions in the ribbon. Note however that from recent analysis of Raman magnon spectra [18] one finds indications for significant interchain superexchange interactions. This interchain exchange is probably also responsible for the disagreement between the frustration parameter determined from these spectra and from susceptibility and other data. Also Kuroe et al [17] find a somewhat larger interchain exchange interaction in the b direction from an analysis of Raman spectra: $J_b = 0.50$ meV. Thus, whether the Cu chain can safely be regarded as a 1D chain remains questionable.

In the SP phase one finds two alternating values for the nn exchange in the Cu chain. This is usual expressed by: $J_{nn}^{\pm} = J(1 \pm \delta(T))$, where J is the average nn exchange interaction in the SP phase, and $J_{nn}^{\pm}$ are the two alternating values. The dimensionless quantity $\delta(T)$ depends on the temperature. From table 2 we see that the estimates of this parameter at $T = 0$ K range from 0.014 to .3, i.e. over one order of magnitude. Gros et al [18] find the best agreement with magnon spectra for an intermediate value.

An important feature of the J_{nn}–J_{nnn} model is that it predicts a spin–gap to develop in the magnetic excitation spectrum for $\gamma > \gamma_c \approx .2412$ [9]. This gap opens irrespective of any lattice distortion. So a singlet spin liquid phase can originate either from the usual SP mechanism or from frustration of the antiferromagnetic order due to a relative strong J_{nnn} exchange interaction.

Based on the preliminary results of a study of the dependence of the exchange constants on the bond angles ([19, 20]) we proposed a microscopic mechanism for the SP transition in $CuGeO_3$: in first approximation we attribute the main lattice changes as due to the change in the soft bond angles especially the angle which the Ge–O bond makes with the CuO_2 ribbon – the *hinge* angle (α), and the Cu–O–Cu *bridge* angle (ϕ) in this plaquette.

In fig. 5 we present a simple picture of this model as applied to the distortion of the

$CuGeO_3$ lattice when pressure is applied along the b–axis. The two basic units of the structure – the CuO_2 ribbon and the GeO_3 chain rotate around the shared O ions: the hinges. This hinge angle has a strong influence on the strength of the nn exchange in $CuGeO_3$. We will see that its influence on the nnn exchange is small.

1.3 The magnetoelastic properties.

So, of interest for our model are the dependencies of these exchange constants on the lattice parameters. Büchner et al (1996) [21] have recently performed a study of the magnetostriction and thermal expansion of $CuGeO_3$ single crystals. They obtained for the pressure dependence of the susceptibility χ along the three principle axes $\delta\chi_{ii}/\delta P_i$ at 60 K: the a–axis -2.5 %/ GPa , the b–axis 5 %/ GPa, and for pressure along the c–axis: 1 %/ GPa. These pressure dependencies are nearly constant from 20 K up to 60 K. Assuming that in the paramagnetic phase at temperatures far above the SP transition temperature, the magnetic susceptibility follows a Curie–Weiss type law, one derives for the variation of the nn exchange in the ribbon with pressure $\delta \ln J_{nn} = 2.3\delta \ln \chi$, so: $\delta \ln J_{nn} = -5.7$, $+11.5$ and $+2.3$ %/GPa, in the a, b and c direction, respectively. We assume that the other exchange contributions are either too small or are independent of pressure.

In order to interpret these magnetoelastic data with structural distortions we have to relate them to elastic data. We use the following elastic constants for an interpretation of these data: $c_{11} = 66$ GPa; $c_{22} = 24$ GPa;$c_{33} = 300$ GPa. We neglect off–diagonal elastic response.

First consider pressure along the b– and c–axes as these are most straightforward to interpret. Assuming that most of the distortions due to the application of pressure are due to changes in the bond angles one finds for pressure along the c–axis, the bridge angle is the softest structural parameter: $\delta\phi/\delta P)_{\text{c axis}} = -0.4^0$/GPa, while for pressure along the b–axis the hinge angle is the most soft structural parameter: $\delta\alpha/\delta P)_{\text{b axis}} = -5^0$/GPa, where the angle $\phi = \angle$(Cu-O-Cu) is the bridge angle, and the angle $\alpha = \angle$(Ge-ribbon) the hinge angle. For their values see table 1. The effect of pressure along the b–axis on the structure is illustrated with a somewhat simplified version of fig. 5 in fig. 6. The

compression of the lattice due to pressure along the b–axis changes the hinge angles α while leaving the bond lengths nearly constant.

Pressure along the b–axis can also cause a slight increase of the bridge angle, but we neglect this response of the lattice; an increase in the bridge angle would cause a decrease of the O2–O2 bondlength, which is already very small and thus very unlikely. Such an increase of the bridge angle would make $CuGeO_3$ more antiferromagnetic, and when we ignore this change in ϕ we even somewhat underestimate the effect P_b on J_{nn}.

Another structural distortion due to pressure along the c–axis would be a buckling of the CuO_2 chain. The effect of such a buckling on the exchange constants is probably small, and antiferromagnetic. So when we ignore this buckling effect we underestimate the effect of P_c on J_{nn}.

The data for pressure along the a–axis are more difficult to translate into changes of a single bond angle. Pressure along this axis would cause probably first a decrease of the van der Waals gap between the layers. The next effect would be a decrease in the thickness of the these layers. This thickness is determined first by the Ge–O–Ge zig–zag chain. So a compression of the layers can be accomplished by stretching the GeO_3 chain which will force an increase of the Cu–O–Cu bridge angles. However like we argued in the previous paragraph this increase of the bridge angle is counteracted by the repulsion of the two O2 bridge ions between two nn Cu ions in the chain. Furthermore, an increase of the tetrahedral angle at The Ge which connects two CuO_2 ribbons will flatten even more the GeO_3 chain. The latter could well lead to an increase in the distance between two Ge neighbors in the a direction. A variation of the hinge angle by a rotation around the O hinges of the two principle subunits is not susceptible directly to the a–axis compression. A simple accordion effect increasing the b–axis, i.e. a rotation around the O hinges, will not help in compressing the system in the a direction.

So altogether one cannot make a straightforward estimate of the change in bridge angles induced by pressure along the a–axis. Assuming that each tetrahedral O–Ge–O angle contributes half of the compression one can make an estimate of the change in the bridge angle. From this we expect that pressure along the a–axis will have an effect

opposite to pressure along the c–axis, which would be about 2 to 3 times as large as the c–axis effect. So we derive an increase of the bridge angle of about 2^0 per GPa pressure along the a–axis. This is about 5 times as large as for applying pressure along the c–axis, while the change in susceptibility is only about 2.5 times as large. From this one might conclude that probably the largest change in the tetrahedral angle is the one connecting two CuO_2 ribbons, i.e. the Ge–O–Ge angle in the b direction, which does not force a change in the bridge angle, and agrees with the earlier argument of constant O2–O2 distance.

For a detailed analysis of these data we refer to Büchner et al (1997) [22]. These data show that the magnetic properties are very sensitive to the hinge angle $\alpha = \angle$ O–O–Ge and bridge angle $\phi = \angle$ Cu–O–Cu, like we predicted [19].

From the above we derive that the nn exchange constant in the ribbon varies with these bond angles as follows. Büchner et al (1997) finds from the shift of the SP transition temperature under applying pressure along the c–axis a change in the nn exchange constant only due to the variation in the bridge angle: $\delta \ln J_{nn}/\delta\phi \approx 5.8$ % $/^0$, and applying pressure along the b–axis a variation in the nn exchange only due to a variation in the hinge angle: $\delta \ln J_{nn}/\delta\alpha \approx 2$ % $/^0$.

This analysis of the variations of the exchange constant with pressure in terms of bond angles are based on the assumption of rigid bond lengths, and that only one soft bond angle varies with pressure applied along each principle direction (b, c). This simple analysis is not applicable for P_a: in this case more than one bond angle is involved.

Another way to derive these variations would be to correlate the angular variation with the change in lattice constant as a function of temperature. For the hinge angle this leads to a twice as large variation and for the bridge angle to nearly the same variation with the lattice parameters. So we suggest that the uncertainty in the angular variation of the nn exchange constant derived above has an error of about 100 % and for the hinge angle a much smaller uncertainty caused by variations in the bridge angle.

Furthermore Büchner et al (1997) find the following approximate relation between the variation of the SP transition temperature and the average susceptibility ($\overline{\chi}$) at 60 K: $[\delta T_{SP}/\delta P_i]/[\delta\overline{\chi}/\delta P_i] \approx 1.5 \pm 0.4\ 10^7$ K g/emu for all directions $i = a$, b, c. Let us assume

that the SP transition temperature is proportional to the exchange constant. Then we have for the linear variation of the nn exchange constant $\delta J_{nn}/\delta P_i = \text{constant} 0.5 \times \delta\chi_{ii}/\delta P_i$, and we find for the relative variations of the exchange constant in the a, b and c direction: $\delta J_{nn} = -1.1 : 2.5 : 0.6$. Above we found for this relative variations from the analysis of the HT susceptibility approximately the same ratios: $-1.1 : 2.2 : 0.45$.

1.4 Superexchange and Structure

As is well–known an exchange between magnetic moments in insulating magnetic compounds based on late transition–metals is predominantly caused by the so–called superexchange. This superexchange is due to the overlap of the localized orbitals of the magnetic electrons with orbitals of intermediate nonmagnetic ligands. There are many processes contributing to superexchange, which appear under various names in various calculational schemes. Nevertheless, usually the sum of these partial processes give results which follow the Goodenough–Kanamori–Anderson (GKA) [24] rules. These rules are based on orbital symmetry considerations and the assumption that the most important covalent bonding is dp_σ. According to these rules a 180^0 superexchange (the magnetic ion–ligand–magnetic ion angle is 180^0) of partially filled d shells with dp_σ bonding, is antiferromagnetic, whereas a 90^0 superexchange is weakly ferromagnetic. This qualitative difference between 180^0 and 90^0 superexchange is due to the fact that, when considering σ bonding only, in the former case the orbitals of the magnetic electrons are overlapping with the same ligand orbital, while in the latter case the magnetic orbitals are overlapping with different mutually orthogonal ligand orbitals. Neglecting direct dd interactions, the molecular orbitals, based on these atomic p and d orbitals, are orthogonal, and so there is only a ferromagnetic superexchange contribution.

Obviously, when π bonding and/or direct dd hybridization become important these rules do not hold anymore. Also when in the 90^0 case the orthogonality of the intermediate ligand orbitals is not strict the GKA rules have to be modified. Such is in fact the case for the nn superexchange along the c–axis in $CuGeO_3$, which has recently been discussed in detail by the present authors [19].

There we have shown that in the case of 90^0 superexchange one should not only take into account the local symmetry of the cation but also the symmetry at the anion position. When valence orbitals of the same type centered at an anion involved in spin transfer between the two cations have different hybridization with a side group, one can have an antiferromagnetic interaction instead of the ferromagnetic one predicted by the GKA rules for 90^0 superexchange.

In principle similar rules hold for the *nnn* superexchange interactions. For the *nnn* superexchange in the *c* direction the spin from one Cu can be transferred over two intermediate O–*p* orbitals to the other *nnn* Cu. In this case the O–*p* orbitals have a finite transfer with both *nnn* magnetic Cu–*d* orbitals. So these *nnn* Cu–*d* orbitals are not orthogonal, and this will lead to an antiferromagnetic superexchange interaction; if there is a finite transfer between two magnetic orbitals, kinetic exchange will usually win from the ferromagnetic direct or potential exchange.

In the case of $CuGeO_3$ there are two such transfer paths (fig. 7) between *nnn*'s along the *c*–axis. It is clear that this leads to a relatively large antiferromagnetic superexchange interaction. In the *nnn* case the ferromagnetic Kramers–Anderson contribution, which is due to two–site cation–*d* anion–*p* exchange and which may cause the pure 90^0 exchange to be ferromagnetic, is much smaller than the antiferromagnetic kinetic superexchange.

In section 2 we consider the *nn* exchange along the *c*–axis, using various schemes: perturbation theory, and an exact diagonalization of a Cu_2O_2 plaquette. The effect of the Ge side group attached to the bridging O pair is taken into account using two approaches.

In the *first*, most simple approach the influence of Ge is taken into account by a shift of one of the *p* orbitals (p_y), and a covalent reduction of the matrix elements containing this orbital. The hinge angle α only appears to describe the effective hybridization between the Ge–sp^3 and this p_y orbitals.

In a *second* approach to describe the influence of the side group Ge on the O–*p* levels we rotate these O-p orbitals of the O–O bridge so that one obtains a σ bonding between O–p_y and the Ge–sp^3 hybrid. The states in the planar Ge–O–O–Ge cluster can easy be diagonalized. This is described in Appendix A.

We study these *nn* and *nnn* exchange interactions as a function of the lattice parameters. We find that perturbation theory, giving quite reasonable results for the exchange constants themselves, is not able to describe their dependence on the bond angles as found from the analysis of the pressure dependence of the magnetic susceptibility. We find that an exact diagonalization of the Cu_2O_2 plaquette is more successful in this respect, and results of this approach can be found in section 3. The reason that the exact diagonalization of the cluster model gives better results compared with the fourth–order perturbation expansion is that in the perturbation approach the angular dependence is mainly caused by the hybridization, the splitting of the levels being constant. In the case of an exact diagonalization the changes in the hybridization are partly compensated by the changes in the level splitting.

Because of the large ratio of the *nnn* and *nn* exchange, the question arises whether one should also take into account an exchange interaction along the *c*–axis with neighbors further away. In order to do this systematically we use a band model for the electronic structure of the nonmagnetic anion states. Such a model has been described by one of the present authors [26]. In this model we only consider two cations at a distance R, each with one nondegenerate half–filled *d*–like state, interacting via a fully–occupied valence band, consisting of mainly anion *p* states. In this case one obtains a closed set of equations in terms of two–particle Green functions. We have taken into account $pp\sigma$ as well as $pp\pi$ bonding. The effect of the Ge side group is easily taken into account within the simple scheme, by shifting the energy of the *p* levels and by introducing a covalent reduction parameter for the matrix elements involving these O–*p* orbitals. In this approach we only calculate the contribution corresponding to the kinetic exchange and correlation exchange mechanism. The contributions stemming from the two–site *dp* exchange and from the anion on–site *pp* exchange are calculated in fourth–order perturbation theory. In section 4 we give a short account of the application of this model to $CuGeO_3$.

In section 2.3 we consider using perturbation theory the exchange interactions along the *a*– and *b*–axis. An estimate of these superexchange constants is of importance because these determine whether one can safely consider $CuGeO_3$ a 1D Heisenberg spin system

or one has also to take into account these superexchange interactions in case they are of comparable magnitude to the ones along the c–axis. The exchange transfer paths are illustrated in fig. 2, and 3. Note first that in both cases there are two exchange transfer paths for the nn interactions, and there is a transfer path to the nnn Cu in both these directions, which partly coincides with the one of the nn transfer paths. Because the O–O bond length is in the a–axis case much longer than in the b–axis case, it is clear that the spin transfer along the b–axis is stronger then along the a–axis. So we expect that the kinetic superexchange interactions between the CuO_2 ribbons in the b direction are larger than in the a direction. In the b direction we expect a weak antiferromagnetic interaction, and in the a direction an even weaker antiferromagnetic or even weak ferromagnetic interaction.

An important clue for the microscopic picture of the SP transition stems from a comparison of the magnetic properties of weak doping by Zn for Cu and Si for Ge. One finds in both cases that a small amount of impurities has an appreciable lowering effect on the SP transition temperature. That small substitutions of Si for Ge has a large effect on the SP transition is at first sight difficult to understand, because Ge and Si ions are only indirectly involved in the nn superexchange interaction in the Cu chains. However closer examination shows that the Si ion has a number of effects on nn superexchange along the c–axis. First, because Si^{4+} has a smaller ionic radius than Ge^{4+}, it causes one of the Cu–O–Cu angles of the CuO_2 plaquette to decrease, and secondly it may increase the Cu–O bond length. Furthermore, this O bonded to Si is taken out of the CuO_2 ribbon plane. This is illustrated in fig. 10. All these small geometrical changes add to a relative large absolute decrease in the kinetic exchange coming from the Cu–O–Cu transfer path to which Si is attached. Due to this relative local distortion of the O–hinge, i.e. the hinges of the accordion model, the accordion motion becomes frustrated. This distortion inhibits an easy rotation of the CuO_2 ribbon w.r.t. the GeO_3 chain. Si is attached to two CuO_2 ribbons and so is twice as effective as Zn on a Cu position to destroy the ordered SP phase. We discuss the consequences of this substitution for nn superexchange in the c direction in section 5.

2 Theory

Let us first discuss the nn exchange interaction along the c–axis because these seem to be of major importance for an understanding of the magnetic properties of $CuGeO_3$. The nn superexchange involves spin exchange over two 90^0 cation–anion–cation transfer paths. Expressions for the various contributions to superexchange for this configuration have been presented before in a discussion of effects due to side groups – bonded to the bridging O ligands of two magnetic cations – on superexchange [19]. There we emphasized especially these side group effects in a more general context. Below we want to apply these ideas in a somewhat more rigorous scheme to $CuGeO_3$. In order to illustrate the method and approximation we use let us consider in some detail the nn 90^0 superexchange along the c–axis in $CuGeO_3$. The Cu ions have a d^9 configuration. The unpaired electron is in a $d_{x^2-y^2}$ orbital as illustrated in fig. 8. On the oxygen we only consider the p_x and p_y orbitals in he ribbon plane. We will only consider σ–type covalent mixing between this Cu–d orbitals and these O–p orbitals. It is defined by $\lambda = t_{dp}/\Delta$, where $\Delta = \epsilon_d - \epsilon_p$, and $t_{pd} = \langle d|H_{eff}|p\rangle$ is the transfer integral.

The influence of the side group Ge is taken into account in two factors. First, by a shift in energy (δ_p) of the atomic O p levels bonded with Ge, and secondly by introducing a covalent reduction parameter η for the various interactions involving this p orbital. In this model we neglect the influence of the p_z orbital hybridization with the Ge sp^3–like hybrid. The p_z is perpendicular to the ribbon plane and so does not participate in the spin transfer process. This model is equivalent to a model in which only the Ge-O bonding levels are taken into account in the spin exchange process. Because of their high energy, the antibonding Ge-O bonds are not participating in the spin exchange process.

In [19] we did not take into account explicitly that Ge is outside the ribbon plane. At room temperature the hinge angle is about 160^0, i.e. about 20^0 out of the ribbon plane. Changes in this angle as a function of temperature, pressure and phase are – as we will see – the principal causes for the changes of the nn exchange interaction along the ribbon. And thus a study of the sensitivity of the exchange interactions for these induced changes in the lattice parameters can be important for an understanding of the mechanism of the

SP transition in $CuGeO_3$.

As we discussed in the introduction, this hinge angle is very susceptible to pressure along the b–axis. In this case the CuO_2 ribbons are rigid units, rotating with respect to the rigid chain of GeO_4 coupled tetrahedra: the accordion model (see fig. 5). The angles and bond lengths within the CuO_2 ribbon and the GeO_4 tetrahedra remain the same while the CuO_2 ribbons rotate around the O shared with the GeO_4 tetrahedra. This is illustrated in fig. 6 where we present a simplified version of this model emphasizing the changes in the hinge angle and the bridge angle. Inspection of fig. 5 makes it clear that there is enough room in the structure for such a rotation of these units with respect to each other.

2.1 The influence of side groups.

In the first approximation one explicitly introduces a mixing of the Ge–sp^3 and O–p orbitals, depending on its angle with the ribbon. We define the Gesp^3–Op_y transfer integral by $V_\sigma = \langle sp^3|H_{eff}|p_y\rangle = \cos(\alpha)\, V_{0\sigma}$, where $V_{0\sigma}$ is the value of this matrix element when Ge is in the ribbon plane. This model is a simple extension of the model presented by the present authors [19]: the hybridization and therefore the covalency factor η depends on the hinge angle α.

In this model the covalency factor defined above is to lowest order

$$\eta = 1/(1 + \delta_p/\delta_\sigma \cos^2(\alpha))^{1/2}, \tag{2.2}$$

where δ_p is the energy shift of the p_y level due to the Ge–O covalency, and δ_σ is the energy difference between the Ge–sp^3 level and the O–p_y level. This factor η is used to correct the matrix elements involving the O–p_y level. For example the pp_σ bonding in the O pair bridge between two Cu in the ribbon, becomes

$$W_\perp = W_{0\perp}\eta^2. \tag{2.3}$$

Also because of this hybridization of the p_y orbitals with the Ge orbitals the Cud–Op, transfer becomes less effective by a factor η.

The usual way to discuss the superexchange interaction for the 90^0 cation–anion–cation configuration is to take the axis of quantization like in fig. 8. In this picture one can easy

see that for 90^0 there is no spin transfer possible between the two cations via dp_σ bonding. For our arguments it is convenient to rotate the axis of quantization as shown in fig. 9. In this picture spin transfer between two *nn* Cu vanishes because of an interference effect: due to the phase difference between transfer via the various possible transfer paths the total *nn* Cu–Cu spin transfer vanishes.

The principal contributions to the *nn* superexchange within this model for the electronic structure are a ferromagnetic contribution due to the spin polarization of the ligand *p* orbitals, caused by one of the Cu spins, interacting with the spin on the other Cu by an two–site *pd* exchange. This gives a ferromagnetic contribution:

$$J_{\rm nn,KA} = -8\lambda^2 J_{pd}, \tag{2.4}$$

A second ferromagnetic contribution comes from the Hund's rule coupling on the O–*p* orbitals, and is proportional to the on–site exchange interaction J_H on the O–*p* orbitals:

$$J_{\rm Hund} = -4\lambda^2 J_H. \tag{2.5}$$

Both these contributions are possible in the 90^0 as well as in the 180^0 cation–anion–cation configuration. In the case of 90^0 the two-site J_{pd} is smaller than in the 180^0 case, because it is in the first case effectively a $dp\pi$–type charge overlap, while in the second case it is a $dp\sigma$–type charge overlap. These two mechanisms are held responsible for the often found ferromagnetic superexchange in the 90^0 case, because as we will see in this limit the antiferromagnetic contributions (nearly) vanish.

When the Cu–O–Cu angle deviates from 90^0 also other mechanisms start to contribute to the *nn* superexchange interaction. The most important are the kinetic and the correlation+ring exchange mechanisms. A brief discussion of these mechanisms can be found in [19] and a detailed account in [26]. A simple derivation gives for the contribution of the kinetic exchange mechanism:

$$J_{\rm kin,nn,c} = -16\left[\lambda_x^2\Delta_x - \lambda_y^2\Delta_y\right]^2/U_d, \tag{2.6}$$

where the excitation energies include the *pp* hybridization $W_\perp$, and the shift δ_p due to the side group Ge: $\Delta_x = \delta_{dp}$, and $\Delta_y = \delta_{dp} + W_\perp + \delta_p$. The covalency parameters include

the geometric factors: $\lambda_x = \lambda \sin(\phi) \sin(\phi/2)$ and $\lambda_y = \lambda\eta \sin(\phi) \cos(\phi/2)$, where η takes into account that part of the p_y orbital is hybridized into an antibonding Ge–O $(sp^3$–$p_y)^*$ orbital. One can easy check that $J_{\rm kin,nn,c}$ vanishes in the case of equivalent p_x and p_y orbitals.

For the correlation and ring exchange mechanism one finds:

$$\begin{aligned} J_{\rm cor,nn,c} &= -16\lambda_x^4\Delta_x^2\left(\frac{1}{2\Delta_x}+\frac{1}{\Delta_{xx}}\right) - 16\lambda_y^4\Delta_y^2\left(\frac{1}{2\Delta_y}+\frac{1}{\Delta_{yy}}\right) \\ &\quad +8\lambda_x^2\lambda_y^2(\Delta_x+\Delta_y)^2\left(\frac{1}{\Delta_x+\Delta_y}+\frac{1}{\Delta_{xy}}\right), \end{aligned} \tag{2.7}$$

where the excitation energies are $\Delta_{\mu\nu} = \Delta_\mu + \Delta_\nu + U_{\mu\nu}$; $U_{\mu\nu}$ is the Coulomb interaction on the ligand p orbitals. The terms with $\Delta_{\mu\nu}$ are contributions involving excitations from one ligand, while the terms with Δ_μ are due to excitations from p orbitals on different ligands. The latter are the genuine ring exchange contributions.

One can show, by expanding $J_{\rm cor,nn,c}$ in $U_{\mu\nu}/(\Delta_\mu + \Delta_\nu)$, that it includes the Hunds rule contribution $J_{\rm Hund}$. The remaining contribution is:

$$J'_{\rm cor,nn,c} = -16(\lambda_x^2\Delta_x - \lambda_y^2\Delta_y)(\lambda_x^2 - \lambda_y^2). \tag{2.8}$$

This contribution also vanishes in the case of equivalent O–p orbitals.

Results of this approach, using the parameters of table 4 are presented in table 5 for various values of the Cu–O–Cu angle, at room temperature and at 20 K and also for both angles ϕ (see table 1) in the SP phase and for the average angle of ϕ in the SP phase. Note that the ratio γ of the nnn and nn exchange is in the region where one expects a significant contribution from spin frustration on the SP transition.

An important parameter in the SP phase is the ratio: $\delta = |J_1 - J_2|/(J_1 + J_2)$. We find approximately $\delta = 0.09$, which is in the range of values found in literature (see introduction).

The gap in the spin wave spectrum in the SP phase is approximately given by: $E_{SG} = 2.1 J_0(\mu)^{2/3}$ [2]. We find $E_{SG} = 1.4$ meV, which is small compared with the experimental value of about 2.1 meV. The deviation from the experimental value can be due to the extra contribution coming from the frustration of the exchange interaction in the CuO_2 ribbon.

2.2 Explicit side group hybridization

Another and probably better way to include Ge is to rotate the axis of quantization of the O–p levels with the rotation of the Ge, so that the O-p_y orbital always points to the Ge–sp^3 hybrids. Here we will not give the details of this approach. It is sufficient to mention that the calculation of the exchange interactions follows the same calculational scheme as for the simple side group approach presented in the previous subsection.

In this approach the covalency parameter η does not change with the $\angle$Ge–(O–O)$_{bridge}$ but one now has to solve for the O-p_y and O-p_z levels explicitly, and neglecting again the Ge–like antibonding $(sp^3$–$p_y)^*$ states one can easily diagonalize the problem. More details can be found in Appendix A.

The results of this attempt to improve the simple side group model presented in the previous section are rather disappointing: the discrepancy between the angular dependence of the nn exchange along the c–axis and experiment increases: they differ by an order of magnitude. We conclude from this that when one accounts only for variations of the transfer matrix elements and but not for the variations in the perturbed energies of the electronic states, one overestimates the angular dependence of the superexchange. Before we give details of a nonperturbational approach, which corrects for this deficiency, we present first results about the superexchange interactions which do not have such a strong angular dependence: the nnn superexchange along the c–axis, and the nn and nnn superexchange in the a and b direction.

2.3 The next-nearest-neighbor exchange interactions.

Let us consider the nnn superexchange along the CuO_2 ribbon shown in fig. 7. We take into account only the pp_σ bonding: $W_\parallel$. Thus we only need to consider the p orbitals directed along the c–axis: the p_x orbitals in this figure. There is no side group effect because these p orbitals are perpendicular to the Ge sp^3 orbitals. The various contributions to the nnn exchange along the c–axis become

- The *kinetic* exchange:

$$J_{\rm kin,nnn,c} = -4\lambda_x^4 \left[\frac{1}{\delta_{dp}+W_\parallel} - \frac{1}{\delta_{dp}-W_\parallel}\right]^2 \delta_{dp}^4/U_d. \tag{2.9}$$

- The *correlation* exchange:

$$\begin{aligned} J_{\rm cor,nnn,c} &= -4\lambda_x^4\delta^4 \left[\frac{1}{(\delta_{dp}+W_\parallel)^2(2\delta_{dp}+2W_\parallel+U_{p_x}/2)} + \frac{1}{(\delta_{dp}-W_\parallel)^2(2\delta_{dp}-2W_\parallel+U_{p_x}/2)} - \right. \\ & \left. 4\,\frac{\delta_{dp}^2}{(\delta_{dp}^2-W_\parallel^2)^2(2\delta_{dp}+U_{p_x}/2)}\right]. \end{aligned} \tag{2.10}$$

- The *ring* exchange contribution:

$$J_{\rm ring,nnn,c} = -2\lambda_x^4\delta_{dp}^4 \left[\frac{1}{(\delta_{dp}+W_\parallel)^3} + \frac{1}{(\delta_{dp}-W_\parallel)^3} - 2\frac{\delta_{dp}}{(\delta_{dp}^2-W_\parallel^2)^2}\right]. \tag{2.11}$$

- The *ferromagnetic* Kramers–Anderson contribution:

$$J_{\rm ferro,nnn,c} = 8\lambda_x^2 \left[\frac{1}{\delta_{dp}+W_\parallel} - \frac{1}{\delta_{dp}-W_\parallel}\right]^2 \delta_{dp}^2 J_{pd,c}, \tag{2.12}$$

  where $J_{pd,c}$ is the two–site dp exchange between the p_x orbital and the $d_{x^2-y^2}$ orbital. We have taken $J_{pd,c} = (J_{p\sigma d\sigma} + J_{p\pi d\sigma})/2$, and we approximate $J_{p\sigma d\sigma} \approx 4J_{p\pi d\sigma}$ in our numerical evaluation of the *nnn* superexchange.

The *total nnn* exchange along the *c*–axis is given by the sum of these contributions:

$$J_{\rm tot,nnn} = J_{\rm kin,nnn,c} + J_{\rm cor,nnn,c} + J_{\rm ring,nnn,c} + J_{\rm ferro,nnn,c}. \tag{2.13}$$

The expressions for the *nn* superexchange interactions in the *a* and *b* direction are equivalent to those for the *nnn* exchange in the *c* direction. Also in this case there are two transfer paths involving two oxygens. One has only to change the definition of some of the parameters in the expressions for the contributions to *nnn* exchange in the *c* direction. Concerning the geometrical factors only the Cu–O–O bond angles and O–O bond lengths are different. In both directions (*a* and *b*) the O–O bond in the transfer paths are in a plane perpendicular to the ribbon. In the *a*–axis case the O–O bond is nearly perpendicular to that of the Ge–O bond: $\tau_a = 82^0$, while for the *b*–axis case this angle is about $\tau_b = 35^0$.

So for the a direction we expect a weak influence of the side group on the superexchange interaction while in the b direction we expect a larger influence of the side group. The reduction factor is:

$$\eta_i = 1/(1 + \delta_p/\delta_\sigma \cos^2(\tau_i))^{1/2}. \tag{2.14}$$

The dp covalency is now given by

$$\lambda_{i,\sigma} = \lambda_{0x}\eta_i \cos(\rho_i)\sin(\phi), \tag{2.15}$$

where ρ_i $(i = a, b)$ is the angle between the O–O pair and the Cu–O bond in the ribbon ($\rho_a = 108^0$, $\rho_b = 111^0$). The factor $\sin(\phi)$ corrects for the fact that the $d_{x^2-y^2}$ is not along the Cu–O bond. Although the two transfer paths to the nn Cu sites in another ribbon are not equivalent concerning their torsion – one Cu–O–O–Cu path has a torsion of 0^0 or 180^0, while the other has a torsion of about 110^0 – this is of no importance for the evaluation of the superexchange when one only takes into account σ bonding.

A peculiarity of the $CuGeO_3$ structure is that in both a and b directions there is exchange to nnn Cu via *one* transfer path which is equivalent with one of the transfer paths to the nn Cu. So the contributions to the nnn superexchange in the a and b direction are the same except for a numerical factor as those for the nn superexchange. Obviously, in the latter case the ring exchange does not contribute. Thus, the expressions for the nnn in the a and b direction can be easily written down.

$$\begin{aligned} J_{\mathrm{i,kin,nnn}} &= J_{\mathrm{i,kin,nn}}/4, \\ J_{\mathrm{i,cor,nnn}} &= J_{\mathrm{i,cor,nn}}/2, \\ J_{\mathrm{i,ferro,nnn}} &= J_{\mathrm{i,ferro,nn}}/2. \end{aligned} \tag{2.16}$$

These two superexchange constants nn and nnn are of the same order of magnitude.

3 Exact diagonalization of the Cu_2O_2 plaquette

In this section we give the results of an exact diagonalization of the Cu_2O_2 plaquette. The set of parameters used in this section are the same as used in the previous sections. We

also take into account the $pp\pi$ bonding, and take for the ratio $W_\pi/W_\sigma = 0.5$.

The side group effect is incorporated in the following way. We neglect in first instance the hybridization of the p orbitals on the O bridge atoms. Then we need to diagonalize only the Ge–O unit. The energy of the sp^3–p_σ bonding state is:

$$\omega = 0.5\left(\Delta_\sigma - \sqrt{\Delta_\sigma^2 + 4V_{0\sigma}^2}\right). \tag{3.17}$$

We obtain the following expression for the covalency parameter:

$$\eta = \left[\sin^2\alpha + a_p^2\cos^2\alpha\right]^{1/2}, \tag{3.18}$$

where a_p is the amount of O–p character in the sp^3–p_σ bond, and α is the hinge angle. The influence of the side group is now taken into account as due to two sources: a geometrical and a chemical one. The first is reflected in the hinge angle α, and the second by the hybridization of the O–p orbitals with the side group (Ge). It is clear that when the hinge angle is 90^0 there is no side group effect, regardless of the strength of the hybridization. The side group effect has a maximum when the hinge angle is 180^0, that is in case the Ge is in the CuO_2 plane.

Using the parameters given in the caption of table 6 we find for the covalency parameter $\eta = 0.925$, and for the shift of the O–p level $\delta_p = 1.65$. We have calculated the change of the nn exchange constant as a function of temperature, accounting for the changes in lattice parameters, and find that it varies from 13.5 meV at 300 K to 13.3 meV at 20 K. We also calculate the nn exchange constants in the SP phase and find: the Cu–Cu dimer exchange is $J_{nn}^+ = 14.04$ meV and for the other nn exchange constant we find $J_{nn}^- = 12.82$ meV, so $|J_{nn}^+ - J_{nn}^-|/(2J) = 0.046$. This is approximately the same value found experimentally. Finally, we calculated the dependence of the nn exchange as a function of the bridge and hinge angle. We find that these are of the right order of magnitude compared with experiment.

4 The band model for the superexchange interactions in the ribbon

For a further understanding and analysis of the magnetic properties of $CuGeO_3$ it is of importance to know whether the further neighbor superexchange interactions in the c direction can be safely neglected. Furthermore we have seen that a perturbation approach is not able to describe the angular dependence of the nn exchange interactions. In the previous section we gave results of an exact treatment of a Cu_2O_2 plaquette, and found results for the dependence of the exchange constants in approximate agreement with experiment. Below we present a model for the calculation of the exchange interaction in which the nonmagnetic (anion) states are represented by bands, and of the cations we only take into account two sites. Basically this is the two–impurity Anderson model applied to non-metals. We also want to study whether a cluster model gives the right order–of–magnitude estimate of the exchange constants and their dependence on the lattice parameters. A band model is more appropriate for a study of the nnn and next nnn exchange interactions than cluster models because it implicitly takes into account transfer paths up to infinite order, and a band model is only limited by the number of orbitals used as a basis for the description of the bands.

A general model of this kind has already been proposed by Geertsma and Haas [26]. We follow this paper (see Appendix B) and give the appropriate expressions for the case of $CuGeO_3$ (see Appendix C). The basic idea of this model is to calculate the superexchange between two magnetic half–filled nondegenerate orbitals which are a distance R apart by considering only their hybridization with fully occupied valence band states, which usually consists mainly out of anion states. The empty conduction band states are neglected. The latter usually consist mainly of cation s states. The d states of the other cations are also neglected. So we have effectively a two–particle system. Spin transfer can only be mediated by excitations from the fully occupied valence states. One can now write down a closed set of integral equations for the two–particle (holes) energies of this system. The energy difference of the singlet and triplet ground state gives the exchange constant ($2J$).

In this model we neglect the ferromagnetic two–site *dp* contribution and the contribution coming from Hund's rule mechanism in the band states. These contributions are calculated in a perturbation scheme, similar to that in section 2.

We proceed as follows. First we calculate the ground state energy of the triplet states using self-consistent second–order perturbation expansion in the *dp* hybridization t_{pd}:

$$\Omega^T = 2(\epsilon_{0d} + U_d - \Gamma(\Omega^T)). \tag{4.19}$$

The expression for the energy shift function Γ can be found in Appendix B (equation B.35). This solution for the triplet state is independent of the interatomic distance between the two Cu. There are also fourth–order t_{pd} contributions, but these are neglected. These can become important when the energy of the ground state in this self–consistent second–order approximation is very close to the band states. This is not the case for $CuGeO_3$.

We find two contributions to the superexchange interaction. One is due to the kinetic spin transfer mechanism in which in the intermediate state two holes are on one of the cations, and the other – the correlation and ring exchange mechanism, in which the two holes are in band states. The kinetic exchange contribution for two Cu at a distance R is:

$$J_{\rm kin}({\rm R}) = 4{\rm S_d}\frac{|\gamma(\Omega^{\rm T},{\rm R})|^2}{{\rm U_d}}, \tag{4.20}$$

where $\gamma(\Omega, R)$, defined by eqn B.36 in Appendix B is the effective *dd* transfer integral between the two Cu–*d* orbitals. It is similar to the transfer integral usually defined in the Hubbard model. In our model the transfer integral is a function of energy. The factor S_d is the amount of d character in the two–particle ground state. This normalization factor is of importance in case of large effective hybridization between the d and band states, i.e. in case when the triplet state Ω^T is close to the top of the valence band.

The correlation and ring exchange contributions are together:

$$J_{\rm cor}({\rm R}) = {\rm S_d}(\Theta^{\rm S}(\Omega^{\rm T},{\rm R}) - \Theta^{\rm T}(\Omega^{\rm T},{\rm R})), \tag{4.21}$$

where Θ is given by eqn B.39 in Appendix B.

The side group effect is taken into account in the same way as in the exact solution for the Cu_2O_2 plaquette discussed in the previous section. Next we calculate the electronic

structure of the O–p bands. The pp transfer matrix elements are defined with respect to their value for a bridge angle of 90^0. Then we can write (see fig. 7):

$$W_{\parallel} = W_{\sigma x} = W/(1+\sin\beta) W_{\perp} = W_{\sigma y} = W/(1-\sin\beta). \tag{4.22}$$

The π bonding is a factor $r = W_{\pi}/W_{\sigma}$ smaller.

Because we cannot include the important ferromagnetic contributions directly in this model, we treat them using perturbation theory. This is permissible in case we calculate the angular dependence of the nn exchange. because these two contributions depend only weakly on the variation of the bridge and hinge angle. For the further neighbor exchange interactions it is less clear whether one can safely use this perturbation scheme for the ferromagnetic Hund's rule and Kramers–Anderson exchange contributions.

The expressions we use for the ferromagnetic exchange due to two–site pd exchange are for the nn contribution

$$J_{nn,ferro} = -8\lambda^2 J_{pd}, \tag{4.23}$$

for the nnn superexchange:

$$J_{nnn,ferro} = -8\lambda^2 \frac{W_{\sigma x}^2}{\epsilon_{0d}^2} J_{pd}, \tag{4.24}$$

and for the next nnn

$$J_{nnnn,ferro} = -8\lambda^2 \frac{W_{\sigma x}^4}{\epsilon_{0d}^4} J_{pd}. \tag{4.25}$$

For the nn Hunds rule contribution

$$J_{nn,Hund} = -4\lambda^4 J_{O,H}, \tag{4.26}$$

for the nnn

$$J_{nnn,Hund} = -4\lambda^4 W_{0x} W_{0y}/\epsilon_{0d}^2 J_{O,H}, \tag{4.27}$$

and for the next nnn

$$J_{nnnn,Hund} = -4\lambda^4 W_{0x}^2 W_{0y}^2/\epsilon_{0d}^4 J_{O,H}. \tag{4.28}$$

For the calculation of the exchange interactions we used a similar set of parameters (see table 6) as used before in the other calculations. The results for the nn and nnn, presented

in table 6, are in remarkable agreement with those from simple perturbation theory, and agree with experiment; the value of the ratio of the nnn and nn superexchange γ thus also agrees with experiment. The dp covalency with the parameters of this table is about 0.24 (calculated as $\sqrt{(1-S_d)/S_d}$). The shift, δ_p, of the O–p level is about 1.65 eV, and $\eta = 0.93$. These values are approximately the same as in the calculations presented in the previous sections.

We have also calculated the nn exchange and the parameter γ as a function of the bridge angle ($\beta = \phi - 90^0$) and hinge angle (α). Results of this study are presented in fig. 11 and fig. 12. For this set of input parameters the dp covalency is nearly independent of these angles. We see that the nn exchange increases by a factor two, from the situation when there is no side group effect ($\alpha = 90^0$) to the expected maximum side group effect ($\alpha = 180^0$). For the chosen set of parameters the nn exchange changes sign for $\beta \approx 0$. The nn exchange has a minimum for $\phi < 90^0$. If our model for the lattice changes induced by pressure along the b–axis is right, then we expect that the hinge angle decreases on applying pressure along the b–axis, and so the nn exchange decreases and the ratio γ of nnn and nn exchange increases.

We have also studied the influence of the chemical bonding factors of the side group. Results are presented in fig. 13 and 14. The nn exchange constant and the ratio γ vary strongly as a function of these chemical bonding factors. The first derivative of the nn exchange with respect to the bridge angle is nearly constant, while its derivative with respect to the hinge angle varies strongly as a function of these chemical bonding factors.

We have also calculated the dependence of the nn exchange on the dp and pp covalency, for the set of parameters of table 6. We find that a 1 % change in these parameters causes a change of about 0.4 (dp) and 0.3 (pp) meV in the nn exchange constant.

We have studied the temperature dependence of the exchange constants. We find that the nn exchange constant varies only slightly in going from 300 to 20 K: it increases by about 0.2 meV. In the SP phase we find a difference of about 1.1 meV between the weak $J^-_{nn} = 13.96$ meV, and strong one $J^+_{nn} = 15.02$ meV. This gives $|J^+_{nn} - J^-_{nn}|/(2J) = 0.037$. This agrees with the ratio obtained from the exact diagonalization of the cluster described

in the previous section.

Finally, we find that the next–*nnn* superexchange is a factor 40 to 100 smaller than the *nnn* superexchange interaction. Thus it is indeed safe to include only first and second neighbor interactions in a chain.

5 Substitution of Si by Ge.

There appeared some puzzling experimental results on the magnetic properties of low Si doped $CuGeO_3$. Compared with the results of low substitution of Zn for Cu, Si is surprisingly even more effective in suppressing the SP phase. For the case of Zn substitution this suppression is obvious, because Zn effectively cuts the magnetic interactions in the Cu chain. For Si this is less obvious. We adopt the following structural model to describe how Si perturbs locally the lattice. We assume that Si substituted for Ge is situated at the original Ge site, and attracts the *nn* O to form a more or less ideal tetrahedron, with bond lengths like found in SiO_2. The part of the lattice of importance in the next discussion is shown in fig. 10. Various hybridization parameters like the *dp*, the *pp* and the sp^3-*p* have to be corrected for the changes in the interatomic distances. Also the change of the geometrical factors in the form of bond angles have to be taken into account. We assume that all other ions remain fixed at their positions.

When we substitute Si for Ge the transfer path (u) between nearest neighbours in the ribbon, with Si as a side group, will differ from that with Ge as a side group (l). So we introduce two *dp* covalency parameters: one for the Si side group: $\lambda_{\mu u}$, and one for the Ge side group: $\lambda_{\mu l}$, where μ refers to the p_x and p_y orbitals on the O. Also the O-*p* Si-sp^3 one-electron excitation energy $\delta_{\mu u}$ differs from that of Ge $\delta_{\mu l}$.

The expressions for the contributions to the *nn* exchange in the ribbon become a somewhat more involved, but can be easy written down, and are in Appendix D. We approximate the dp_π covalency by: $\lambda_\pi = \lambda_\sigma/3$. For the two one–site *dd* exchange integrals we take 1 eV.

The Si–O bond length is about .13 $\AA$ smaller than that of Ge–O. Within the model for the deviation proposed above we find that $\beta_u \approx 3^0$, and that the Cu–O and $(O–O)_{bridge}$

become both about 10 % larger: $t_{pdu} \approx .9t_{pd}$, $J_{pdu} \approx .9J_{pd}$ and $W_\perp \rightarrow 0.9W_\perp$. We neglect the slight deviation from planarity of the Cu_2O_2 plaquette.

As a result we find that $J_{c,nn} \approx 0 \pm 0.5$ meV. So Si destroys the nn superexchange in the Cu_2O_2 plaquette. The only coupling that remains is the nnn over the plaquette. Compared with Zn, Si will be more effective in destroying the nn coupling, because it is attached to two ribbons. Another factor which may influence the doping dependence of the SP transition is that Zn and Si act differently on the frustration: if one takes into account the nnn exchange interaction, a Zn–doped chain will be still totally antiferromagnetic (albeit with weakened AF exchange between Cu's across Zn), whereas Si, with the J_{nnn} included will render the corresponding bond either completely frustrated, or even ferromagnetic. It is this factor which possibly explains why Si doping is not twice but even three times more effective in suppressing the SP phase than the Zn ones [27]

6 Discussion.

The fourth–order perturbation expansion usually used in the calculation of superexchange constants, is also successful in the case of the various exchange interactions in $CuGeO_3$. We find good agreement of our calculations with experiment. We find a value for the frustration parameter (see table 5) which is in the range of values found in literature (see table 2). Also the values for the two alternating exchange constants in the SP phase is in the range of values found in the literature (see also table 2. The exchange in the a and b direction are in our perturbation scheme nearly two orders of magnitude smaller than the nn exchange in the c direction.

However the results for the angular dependence of the nn superexchange using this perturbation approach differ by nearly an order of magnitude from the experimental data. Also further refinements in the treatment of the O–O bridge and the hybridization between these O and the Ge side group give no improvement; on the contrary, the disagreement for the angular dependence with experiment increases.

In this perturbation scheme the transfer matrix elements depend on these angles. In the formulation of the superexchange these are the only ingredients which depend on the

angle. The excitation energies do not depend on the transfer integrals. However, we know that in general these also may depend on the size of the transfer integrals. This is usually neglected, and the transfer integrals and excitation energy are taken from some tight–binding fit to an electronic bandstructure or cluster calculation, so that actually one takes the energy of the perturbed states: one thus renormalizes the excitation energies. The energy differences of these perturbed states have a second order dependence on the transfer integrals.

When the unperturbed energy differences are of the same order as the transfer integrals, these energies become very sensitive to changes in the transfer integrals. This is actually the case in $CuGeO_3$.

In order to take into account simultaneously changes in matrix elements and in the excitation energies, we perform an exact diagonalization of a Cu_2O_2 cluster, using essentially the same model as in the perturbation approach. We calculated the energy difference of the singlet and triplet state. In this approach the results for all exchange interactions and the dependence of the nn exchange on the bond angles compare well with available experimental data. The shift in excitation energy due to the change in bond angles compensates partly the change in the transfer integrals. The consequence is that the nn exchange in the ribbon is much less sensitive to changes in the lattice parameters.

We obtain rather small – nearly two orders of magnitude smaller than the nn exchange in the c direction – values for the exchange in the a and b direction. We also find a rather small next–nnn exchange in the c direction from our solution of the band model. Thus from our calculation it follows that one can view this compound as a frustrated 1D spin system with nn and nnn exchange in the c direction.

We calculated the consequences of the substitution of Ge by Si, using the perturbation approach. Due to the decrease in the bridge angle ϕ, and the increase in the hinge angle β the nn exchange in the ribbon decreases strongly. We know that the perturbation approach overestimates the sensitivity of exchange for these lattice changes. However even a much smaller change in the nn exchange, for example a decrease by only 50 %, would have drastic consequences, because such a value would effectively frustrate the exchange interaction:

nn and *nnn* exchange then become approximately the same, which may introduce kink in the long–range order.

The values for the alternating exchange constant in the SP phase are of the right order of magnitude; note however that the analysis of the experimental data give values which differ by an order of magnitude (see discussion in the introduction).

Another consequence of this model is an elastic one. The rotation of the two 1D sublattices CuO_2 and GeO_3 around the shared oxygen becomes frustrated in case of substitution of Si for Ge: the Si–O bond is shorter than the Ge–O bond. Rotation of these two units would then also involve a change in the Cu–O bondlengths: increase of the hinge angle would increase the Cu–O bond length, in order to accommodate the Si–O bond length. Thus we expect that Si doped $CuGeO_3$ shows a less strong dependence of the susceptibility on applying pressure along the *b*–axis.

7 Summary and Conclusions.

In this paper we carried out microscopic calculations of the exchange constants in $CuGeO_3$ and studied their dependence on the lattice parameters. Our treatment in this paper allows to explain many features of this compound, which at first glance look rather puzzling, such as the observed sensibility for pressure applied perpendicular to the CuO_2 ribbons, and the sensitivity of the *nn* exchange along the *c*–axis to Si doping

We show how the account taken of the local geometry and the side groups Ge and Si lead to a rather detailed microscopic picture of the distortions in $CuGeO_3$, both above and below the SP transition. These results are largely specific for this particular compound, although some of the conclusions (for example the role of side groups in superexchange and the importance of soft bond bending modes) are of a more general nature.

We conclude that a perturbation approach is valid for the calculation of the superexchange parameters for a fixed set of lattice parameters, but when one wants to study the dependence of these exchange parameters on the lattice parameters one has to take into account also the shift of the energy levels. Only in the limit of very ionic compounds these shifts are too small to be of significance. A cluster model – in our case Cu_2O_2 – and also

a band model for the anion (O) states give results that compare well with experiment.

We conclude also that the nn exchange in the CuO_2 ribbon is most sensitive to changes in the hinge angle. The other exchange interactions, in the ribbon and between ribbons, are rather insensitive to the side group Ge. The sensitivity of the nn exchange to the changes in the lattice is due to the strong interference effects which are not present in the case of the other exchange interactions: nnn in c direction, and nn in the a and b direction. This sensitivity to the side groups is also the cause of the large influence of Si substitution on the nn exchange.

The presence of the two one–dimensional sublattices: the CuO_2 ribbon and the GeO_3 chain, which can easy rotate with respect to each other around the shared O ions – the accordion model – is the basis for the understanding of the properties of this inorganic spin–Peierls compound.

acknowledgments

The first author thanks CNPQ for a grant – number: 300920/97-0 – to complete this work. The work of D. Khomskii was supported by the Netherlands Foundation for Fundamental Study of Matter (FOM) and by the European Network OXSEN.

A Explicit side group treatment.

In this appendix we give the expressions for the covalency parameters in case we take into account explicitly the O-Ge σ hybridization. On the Ge we only consider a sp^3 hybridized orbital pointing in the direction of the O in the ribbon, hybridizing with the O–p_y orbital. The O–p_x orbital points along the ribbon, and therefore the O–p_x orbital are not hybridizing with the sp^3 hybrids. We neglect again pp_π bonding. For more details see the main text. Note that we now also have to include the p_z orbitals on the O, because they have a component in the CuO_2 ribbon plane. The p_x are not affected, these remain in the ribbon, perpendicular to the Ge-sp^3 hybrid. Because all three p orbitals of O can now participate in the spin transfer process, the number of covalency parameters increases from 2 to 3.

In this approximation the dp_σ covalency parameters λ_x , λ_y and λ_z can be written as:

$$\begin{aligned} \lambda_x &= \lambda_{0x}\sin(\phi)\sin(\phi/2), \\ \lambda_y &= \lambda_{0y}\sin(\phi)\cos(\phi/2)\cos(\alpha)\eta_0, \\ \lambda_z &= \lambda_{0z}\sin(\phi)\cos(\phi/2)\sin(\alpha), \end{aligned} \tag{A.29}$$

where $\lambda_{0\mu} = t_{dp\sigma}/\Delta_\mu$ ($\mu = x,\ y,\ z$), and where Δ_μ is the energy difference between the d_{xy} orbital and p_μ: $\Delta_x = \delta_{dp}$, $\Delta_y = \delta_{dp} + \delta_p + W_y$ and $\Delta_z = \delta_{dp} + W_z$. Furthermore the pp_σ transfer is for the bridging O pair: $W_y = W_\perp \eta_0^2 \cos^2(\alpha)$ and $W_z = W_\perp \sin^2(\alpha)$. The covalency parameters λ_y and λ_z depend on the angle $\alpha = \angle(\text{Ge–(O–O)}_{\text{pair}--\text{bridge}}$. When this angle is 90^0, λ_y vanishes, because Ge is perpendicular to the Cu_2O_2 plaquette. In this case there is no side group effect. When $\alpha = 180^0$, λ_z vanishes, because Ge is in the plane of the plaquette. In this limit the side group effect has a maximum.

In order also to take into account the change in the O–O pair bond length, we define W as the transfer integral in case that the $\angle$ Cu–O–Cu is 90^0. For the pp hybridization we assume a R^{-2} scaling, and for the dp we assume a R^{-3} scaling So for the deviation from 90^0, given by β, and assuming that the Cu–O bond length does not change we can write for the pp transfer integral of the O–O pair bridge,

$$W_\perp = W/(1 - \sin(\beta)), \tag{A.30}$$

and for later use the pp_σ transfer along the ribbon

$$W_\parallel = W/(1+\sin(\beta)). \tag{A.31}$$

B Two impurity Anderson Model for Superexchange in Non metals

In this appendix we give the expressions for the various functions appearing in equations for superexchange in $CuGeO_3$ in the two–impurity Anderson Model. In this model the nonmagnetic states are described by band states, and the magnetic states by localized d–like functions. The hybridization between these two kind of states is $t_{d\mathbf{k}}$. The only Coulomb interaction one takes into account is the on–site Coulomb interaction U_d on the two magnetic ions.

The basic equations for the electronic structure and the exchange interactions can be found in [26]. There are two contributions to superexchange: the kinetic superexchange and the correlation exchange. The latter includes the ring exchange contribution. The ferromagnetic contributions due to the Hund's rule coupling in the nonmagnetic states and the ferromagnetic due the exchange coupling between the band and localized states do not appear in this model.

The expression for the kinetic exchange up to fourth order in the $d\mathbf{k}$ hybridization is for two d orbitals 1 and 2 at a distance R:

$$J_{kin} = 2\left(\Gamma(\Omega^S) - \Gamma(\Omega^T)\right) + 4\frac{|\gamma_{12}(\Omega^S|^2}{\Omega^S + 2\epsilon_{0d} + U_d - \Gamma(\Omega^S)}, \tag{B.32}$$

where the triplet energy is given by the solution of:

$$\Omega^T = -2\left(\epsilon_{0d} + U_d - \Gamma(\Omega^T)\right), \tag{B.33}$$

and the singlet energy is given by the solution of

$$\Omega^S = -2(\epsilon_{0d} + U_d - \Gamma(\Omega^S)) - 2\frac{|\gamma_{12}(\Omega^S)|^2}{\Omega^S + 2\epsilon_{0d} + U_d - \Gamma(\Omega^S)}. \tag{B.34}$$

The energy of the triplet state is in this contribution independent of the distance between the cations, while the energy of the singlet state depends on the distance between the two

atoms. The second–order energy shift is:

$$\Gamma(\Omega) = \sum_{\mathbf{k}} \frac{|t_{d\mathbf{k}}|^2}{\Omega + \epsilon_{0d} + U_d + \epsilon_{\mathbf{k}}}, \tag{B.35}$$

and we have defined:

$$\gamma_{12}(\Omega) = \sum_{\mathbf{k}} \frac{t_{1\mathbf{k}} t_{\mathbf{k}2}}{\Omega + \epsilon_{0d} + U_d + \epsilon_{\mathbf{k}}}, \tag{B.36}$$

where the sum over $\mathbf{k}$ also is over the bands.

An expansion around the lowest triplet energy determined from equation B.33 gives for this kinetic energy contribution for two d orbitals 1 and 2 at a distance R:

$$J_{kin}(R) = 4S_d \frac{|\gamma_{12}(\Omega^T|^2}{U_d}, \tag{B.37}$$

where S_d is the total d character in the particle triplet ground state. It is given by

$$S_d = 1/(1 - 2\,\frac{\delta\Gamma(\Omega)}{\delta\Omega}\Big|_{\Omega=\Omega^T}). \tag{B.38}$$

Especially in covalent systems, where the perturbed partially filled localized states are near the top of the fully occupied valence band, this factor is important to obtain good agreement between an exact solution and this approximate expansion.

The energy of the two–particle singlet and triplet states including the correlation and ring exchange mechanism are up to fourth order for two d states 1 and 2 determined by the following integral equations:

$$\begin{aligned}\Omega^{S/T} &= -2(\epsilon_{0d} + U_d - \Gamma(\Omega^{S/T})) - \sum_{\mathbf{k},\mathbf{l}} \left[\left(\frac{1}{\Omega^{S/T} + \epsilon_{\mathbf{k}} + \epsilon_{0d} + U_d} + \frac{1}{\Omega^{S/T} + \epsilon_{\mathbf{l}} + \epsilon_{0d} + U_d} \right)^2 \right. \\ &\left. \frac{|t_{1\mathbf{l}}|^2 \, |t_{2\mathbf{k}}|^2 \pm t_{2\mathbf{l}} t_{\mathbf{l}1} t_{1\mathbf{k}} t_{\mathbf{k}2}}{\Omega^{S/T} + \epsilon_{\mathbf{k}} + \epsilon_{\mathbf{l}}} \right],\end{aligned} \tag{B.39}$$

where the +/- apply to the singlet/triplet state. Let us denote the sum over $\mathbf{k}, \mathbf{l}$ in the rhs of this expression by $\Theta^{S/T}$. We assume that the exchange constant is much smaller than any of the excitation energies. We may expand the energy of the singlet state around the triplet state energy given by equation B.33, and we obtain for the correlation contribution to the superexchange interaction:

$$J_{cor}(R) = S_d(\Theta_{12}^S - \Theta_{12}^T), \tag{B.40}$$

which can be further approximated by

$$J_{cor}(R) = 2S_d \sum_{\mathbf{k},\mathbf{l}} \left[\left(\frac{1}{\Omega^T + \epsilon_{\mathbf{k}} + \epsilon_{0d} + U_d} + \frac{1}{\Omega^T + \epsilon_{\mathbf{l}} + \epsilon_{0d} + U_d} \right)^2 \frac{t_{2\mathbf{l}} t_{\mathbf{l1}} t_{1\mathbf{k}} t_{\mathbf{k2}}}{\Omega^T + \epsilon_{\mathbf{k}} + \epsilon_{\mathbf{l}}} \right]. \quad \text{(B.41)}$$

Using one single orbital for the sum over $\mathbf{k}$ and $\mathbf{l}$ one can easily check that this leads to the usual expression for the correlation exchange contribution for a three center cation–anion–cation cluster model. Also one can check easily that it includes the ring exchange contribution.

C Application to $CuGeO_3$

In the case of $CuGeO_3$ we only consider the CuO_2 ribbons.

The band states are described by $\epsilon_{\mu\mathbf{k}}$. where μ is a band index. The unperturbed d states d_1 and d_2 have an energy ϵ_{0d}. We only consider the O–p orbitals p_x, p_y in the CuO_2 ribbon plane. We take into account the $pp\sigma$ as well as the $pp\pi$ hybridization. These split up into four bands, of which only two are interacting with the d_{xy} orbitals. The linear combinations are:

$$p_{x^-} = (p_{xu} - p_{xl})/\sqrt{2}; \qquad p_{y^+} = (p_{yu} + p_{yl})/\sqrt{2}, \quad \text{(C.42)}$$

where the subscript u and l refer to the upper and lower O chain. The energies of these two linear combinations are:

$$\epsilon^- = \epsilon_{px} = \epsilon_{0px} + W_{\pi x}; \qquad \epsilon^+ = \epsilon_{py} = \epsilon_{0py} - W_{\sigma y}. \quad \text{(C.43)}$$

The $W_{\sigma y}$ also contains a covalent factor η which takes into account the hybridization of the p_y orbital with the side group orbitals in our case the sp^3 hybrids of Ge. Also the energy of the p_y orbital is shifted by an amount δ_p due to this Ge–O hybridization. So $\epsilon_{0py} = \epsilon_{0px} + \delta_p$. For the pp hybridization we assume a R^{-2} scaling, and for the dp we assume a R^{-3} scaling. Both $W_{\pi x}$ and $W_{\sigma y}$ depend on the bridge angle ϕ. Expressed in terms of their value for the case $\phi = 180^0$, we can write for these two parameters:

$$W_{\sigma x} = W_0/(1 - \sin\beta); \qquad W_{\sigma y} = W_0/(1 + \sin\beta). \quad \text{(C.44)}$$

For convenience we define the following quantities:

$$g_x = [\sin(\phi)\cos(\phi/2)]^2; \qquad g_y = [\eta\sin(\phi)\sin(\phi/2)]^2. \tag{C.45}$$

These expression contain the geometrical factors: the bridge angle ϕ, and the influence of the side group is represented by the covalency factor η. The energy shift functions for the two bands read:

$$\Gamma_{x^-}(\Omega) = \frac{8t_{pd}^2}{2\pi} g_x \int_0^\pi \frac{1+\cos k}{\Omega + \Delta_x(k)} dk, \tag{C.46}$$

$$\Gamma_{y^+}(\Omega) = \frac{8t_{pd}^2}{2\pi} g_y \int_0^\pi \frac{1-\cos k}{\Omega + \Delta_y(k)} dk, \tag{C.47}$$

and the total shift is

$$\Gamma(\Omega) = \Gamma_{x^-}(\Omega) + \Gamma_{y^+}(\Omega), \tag{C.48}$$

where we have defined:

$$\Delta_x(k) = \epsilon_x + W_{\sigma x}\cos k; \qquad \Delta_y(k) = \epsilon_y - W_{\pi y}\cos k,$$
$$\epsilon_x = \epsilon_{0d} + U_d + \epsilon_{0px} + W_{\pi x}; \qquad \epsilon_y = \epsilon_{0d} + U_d + \epsilon_{0py} + W_{\sigma y}. \tag{C.49}$$

The kinetic transfer for two d_{xy} orbitals at a distance $R = cn$, where n is an integer, and c the nn Cu–Cu distance in the ribbon, is determined by the function:

$$\gamma_{x^-}(\Omega, n) = \frac{8t_{pd}^2}{2\pi} g_x \int_0^\pi \frac{(1+\cos k)\cos kn}{\Omega + \Delta_x(k)} dk,$$
$$\gamma_{y^+}(\Omega, n) = \frac{8t_{pd}^2}{2\pi} g_y \int_0^\pi \frac{(1-\cos k)\cos kn}{\Omega + \Delta_y(k)} dk, \tag{C.50}$$

and the total kinetic transfer is

$$\gamma(\Omega, n) = \gamma_{x^-,n}(\Omega) + \gamma_{y^+,n}(\Omega). \tag{C.51}$$

The total kinetic energy shift is

$$\Theta_{kin}(\Omega, k) = 4\frac{|\gamma(\Omega, n)|^2}{\Omega + 2\epsilon_{0d} + U_d - \Gamma(\Omega)}. \tag{C.52}$$

The correlation energy shifts are for the singlet and triplet state:

$$\Theta_{xx}^{S/T}(\Omega, n) = \int_{-\pi}^{\pi} dk \int_0^\pi dl \frac{(1+\cos k)(1+\cos l)(1 \pm \cos(k-l)n)}{\Omega + \Delta_{xx}(k,l)} \left(\frac{1}{\Omega + \Delta_x(k)} + \frac{1}{\Omega + \Delta_x(l)}\right)^2,$$

$$\Theta_y^{S/T}(\Omega,n) = \int_{-\pi}^{\pi} dk \int_0^{\pi} dl \frac{(1-\cos k)(1-\cos l)(1\pm\cos(k-l)n)}{\Omega+\Delta_{yy}(k,l)} \left(\frac{1}{\Omega+\Delta_y(k)}+\frac{1}{\Omega+\Delta_y(l)}\right)^2,$$
$$\Theta_{xy}^{S/T}(\Omega,n) = \int_{-\pi}^{\pi} dk \int_0^{\pi} dl \frac{(1+\cos k)(1-\cos l)(1\pm\cos(k-l)n)}{\Omega+\Delta_{xy}(k,l)} \left(\frac{1}{\Omega+\Delta_x(k)}+\frac{1}{\Omega+\Delta_y(l)}\right)^2. \quad \text{(C.53)}$$

The $+$, $-$ sign applies to the singlet (S) and triplet (T) state respectively. The total correlation energy shift is for the S/T two particle state:

$$\Theta^{S/T}(\Omega,n) = 2\frac{t_{pd}^4}{\pi^2}\left[g_x^2\Theta_{xx}^{S/T}(\Omega,n)+g_y^2\Theta_{yy}^{S/T}(\Omega,n)+2g_xg_y\Theta_{xy}^{S/T}(\Omega,n)\right]. \quad \text{(C.54)}$$

From this quantity for $n = 1$, 2 and 3 we calculate the nn, nnn and next nnn superexchange interactions.

D The equations for the nn exchange with Si substitution.

In this appendix we give the expressions for the nn exchange in the c direction in case Si is sunstituted for one of the Ge side groups.

The *ferromagnetic dp* contribution is given by:

$$\begin{aligned} J_{\text{ferro}} &= 4[\lambda_{0xl}^2\cos^6(\beta_l)+\lambda_{0xu}^2\cos^6(\beta_u)]J_{d\sigma p\pi} \\ &\quad +4[\lambda_{0xl}^2\sin^2(\beta_l)\cos^4(\beta_l)+\lambda_{0xu}^2\sin^2(\beta_u)\cos^4(\beta_u)]J_{d\sigma p\sigma}, \end{aligned} \quad \text{(D.55)}$$

where we have neglected the $J_{d\pi p\pi}$ and the $J_{d\pi p\sigma}$ proportional to $\sin^4(\beta)$.

The *kinetic* exchange contribution is

$$J_{\text{kin}} = -4/U_d\left[\lambda_{xl}^2\Delta_{xl}+\lambda_{xu}^2\Delta_{xu}-\lambda_{yl}^2\Delta_{yl}-\lambda_{yu}^2\Delta_{yu}\right]^2. \quad \text{(D.56)}$$

There are two contributions to the correlation exchange. The first one involves a double excitation on one O and one p level, and gives

$$J_{\text{cor},1} = -8\lambda_{xu}^4\Delta_{xu}^2/D_{xxu}-8\lambda_{xl}^4\Delta_{xl}^2/D_{xxl}-8\lambda_{yu}^4\Delta_{yu}^2/D_{yyu}-8\lambda_{yl}^4\Delta_{yl}^2/D_{yyl}. \quad \text{(D.57)}$$

The second contribution is due to the double excitation from two p levels on the same O:

$$J_{\text{cor},2} = 4\lambda_{xu}^2\lambda_{yu}^2(\Delta_{xu}+\Delta_{yu})^2/D_{xyu}+4\lambda_{xl}^2\lambda_{yl}^2(\Delta_{xl}+\Delta_{yl})^2/D_{xyl}. \quad \text{(D.58)}$$

Finally we have the *ring* exchange contribution, which is given by the double excitation from p orbitals on different O of the O pair bridge. One obtains:

$$J_{\rm ring} = -4\lambda_{xu}^2\lambda_{xl}^2(\Delta_{xu}+\Delta_{xl})-4\lambda_{yu}^2\lambda_{yl}^2(\Delta_{yu}+\Delta_{yl})-4\lambda_{xu}^2\lambda_{yl}^2(\Delta_{xu}+\Delta_{yl})-4\lambda_{yu}^2\lambda_{xl}^2(\Delta_{yu}+\Delta_{xl}). \tag{D.59}$$

Note that these correlation contributions already contain the contribution due to Hunds rule.

Next to these contributions there appear two new ferromagnetic contributions due to a kinetic transfer mechanism. The contributions vanish in the case that the transfer paths along the two bridge O are the same. In the case of a single Si substitution the upper (via the O bonded to Si) and lower (bonded to Ge) transfer paths are inequivalent, The two contributions which appear are due to Hunds rule coupling on the Cu: one due to d_π–d_σ and the other due do d_{σ_1}–d_{σ_1} on–site exchange.

We find for these contributions:

$$J_{nn\pi\sigma} = 4\left[(\lambda_{xu}\lambda_{\pi xu}+\lambda_{yu}\lambda_{\pi yu})\Delta_u-(\lambda_{xl}\lambda_{\pi xl}+\lambda_{yl}\lambda_{\pi yl})\Delta_l\right]^2\left(\frac{J_{\pi\sigma}}{U_d}\right)^2, \tag{D.60}$$

and

$$J_{nnz^2,x^2-y^2} = 4\left[(\lambda_{xu}\lambda_{z^2xu}+\lambda_{yu}\lambda_{z^2yu})\Delta_u-(\lambda_{xl}\lambda_{z^2xl}+\lambda_{yl}\lambda_{z^2yl})\Delta_l\right]^2\left(\frac{J_{z^2,x^2-y^2}}{U_d}\right)^2. \tag{D.61}$$

References

[1] M. Braden, G. Wilkendorf, M. Aïn, G. J. McIntire, M. Behruzi, G. Heger, G. Dhalenne and A. Revcolevschi, *Phys. Rev. B* **54)**, 1105 (1996) .

[2] M. Cross and D. S. Fisher, *Phys. Rev.* **19**, 402 (1979) ; M. C. Cross, *ibid.* **20**, 4606 (1979).

[3] J. C. Bonner and M. E. Fisher, *Phys. Rev. A* **135**, 640 (1964).

[4] H. Kuroe, K. Kobayashi, T. Sekine, Y. Hase, M. Sasago, I. Terasaki and K. Uchinokura. *J. Phys. Soc. Jpn.*, **63**, 365–6 (1994).

[5] M. Hase, I. Terasaki, Y. Sasago, K. Uchinokura, and H. Obara, *Phys. Rev. Lett.*, **71**, 4059–62 (1993).

[6] M. Nishi, O. Fujita, and J. Akimitsu, *Phys. Rev. B*, **50**, 6508 (1994).

[7] H. Nojiri, T. Hamamoto, Z. J. Wang, et al., *J. Phys. Condens. Matter* **9**, 1331–1338 (1997) .

[8] R. A. Cowley, B. Lake and D. A. Tannent, *J. Phys. Condens. Matter*, **8**, L179–L185 (1996).

[9] G. Castilla, S. Chakravarty and V. J. Emery, *Phys. Rev. Lett.*, **75**, 1823–1826 (1995).

[10] J. Riera and A. Dobry, *Phys. Rev. B* **51**, 16098 (1995).

[11] J. Riera and S. Koval, *Phys. Rev. B* **53**, 770 (1997).

[12] M. Arai, M. Fujita, M. Motokawa, J. Akimitsu and S. M. Bennington, *Phys. Rev. Lett.* **77**, 3649–3652 (1997).

[13] P. H. M. van Loosdrecht, J. Zeman, G. Martinez, G. Dhalenne and A. Revcolevski, *Phys. Rev. Lett.* , **78**, 487–489 (1997).

[14] M. Hase, Y. Sasago, I. Terasaki, K. Uchinokura, G. Kido and T. Hamamoto, J. Phys. Soc. Japan, **65** 273 (1996).

[15] K. Fabricius, A. Klümper, U. Löw, B. Büchner and T. Lorenz, cond-mat/9705036.

[16] H. Kuroe, J.–I. Sasaki, T. Sekine, N. Koide, Y. Sasago, K. Uchinokura and M. Hase, *Phys. Rev. B* **55**, 409–415 (1997).

[17] H. Kuroe, T. Sekine, M. Hase, Y. Sasago, K. Uchinokura, H. Kojima, and I. Tanaka and Y. Shibuya, Phys. Rev. B **50**, 16468-16473 (1994).

[18] C. Gros, W. Wenzel, A. Fledderjohann, P. Lemmens, M. Fischer, G. Güntherodt, M. Weide, C. Geibel, F. Steglich, cond-mat:961201.

[19] W. Geertsma and D. Khomskii, *Phys. Rev. B* **54**, 1105–1116 (1996).

[20] D. Khomskii, W. Geertsma and M. Mostovoy, *Czech. J. Phys.*, **46**, 3239 (1996).

[21] B. Büchner, U. Ammerdahl, T. Lorenz, W. Brenig, G. Dhalenne and A. Revcolevski, *Phys. Rev. Lett.* **77** 1624–1627 (1996).

[22] B. Büchner et al., *Phys. Rev. B* (1997).

[23] B. Büchner, private communication.

[24] J. Goodenough, *Magnetism and the Chemical Bond*. John Wiley and Sons, New York, London, (1963).

[25] W. Geertsma, *Physica B*, **164**, 241–260 (1990).

[26] W. Geertsma and C. Haas, *Physica B*, **164**, 260–286 (1990).

[27] B. Grenier, J.–P. Renard, P. Veillet, C. Paulsen, G. Dhalenne and A. Revcolevski, *Phys. Rev. B*, **58** 8202 (1998).

Table 1: Structure details relevant for the calculation of the various superexchange interactions. Data are from [1].

Bond/angle	300 K	20K	4.2 K
Cu–O2	1.9326	1.9327	1.9351/1.9322
(O2–O2) $_{\text{perp.chain}}$	2.5089	2.504	2.4984/2.5159
$(\text{Ge–O1})_{\text{chain}}$	1.7730	1.7761	1.742
$\text{Cu–O1}_{\text{apical}}$	2.7549	2.7295	2.7300
$(\text{O2–O2})_{\text{a--axis}}$	3.062	3.028	
$(\text{O2–O2})_{\text{b--axis}}$	2.8249	2.825	
$(\text{O2–O2})_{\text{par.chain}}$	2.9404	2.9445	
$\alpha = \angle\text{Ge–}(\text{O–O})_{\text{c--bridge}}$	159.52	158.85	159.86/158.10
$\phi = \angle(\text{Cu–O–Cu})_{\text{ribbon}}$	99.06	99.24	99.56/98.76
$\tau_a = \angle\text{Ge–}(\text{O–O})_{\text{a--bridge}}$	82.00	81.55	
$\tau_b = \angle\text{Ge–}(\text{O–O})_{\text{b--bridge}}$	35.38	35.49	
$\rho_a = \angle(\text{O–O})_{\text{c--bridge}}\text{–O}_{\text{apath}}$	118.48	119.62	
$\rho_b = \angle(\text{O–O})_{\text{c--bridge}}\text{–O}_{\text{bpath}}$	124.14	123.35	
$\theta_a = \angle(\text{O–O})_{\text{a--bridge}}\text{–Cu}$	108.03	108.67	
$\theta_b = \angle(\text{O–O})_{\text{b--bridge}}\text{–Cu}$	111.36	110.81	
$\angle_{\text{torsion}}(\text{Cu–}(\text{O–O})_a\text{–Cu})$	72.95 (1×)		
	180.0 (1×)		
$\angle_{\text{torsion}}(\text{Cu–}(\text{O–O})_b\text{–Cu})$	109.22 (1×)		
	0.00 (1×)		

Table 2: Some experimental values for the exchange constants in $CuGeO_3$, all in meV. The parameters are defined by the equation 1.2.

J_{nn}	J_{nnn}	J_a	J_b	γ	$\delta(0)$	method reference
-10.4	–	0.044	-0.35	–	–	Magn. Suscept.; [4]
-7.6	–	–	–	–	0.17	Magn. Suscept.;[5]
-10.4	–	0.1	-1.0	–	0.12	Inel.Neutron Scat.; [6]
-15.5	–	–	–	–	–	Magn. sat.; [7]
-11.9	–	–	–	–	–	Low field magn.; [14]
-5.8	-4.9	0.00±0.03	-0.315	0.86	–	Magnon disp.; [8]
-13.0	-3.1	–	–	0.24	0.03	HT Magn. Suscept.+ LT Magnon dispersion; [9]
-13.8	-4.9	–	–	0.36	0.014	HT Magn. Suscept.; [10],[11]
-12.8	-6.6	–	–	0.51	–	Inel. Neutron Scat.; [12]
-15.5	-2.8	–	–	0.18	–	Raman; [13]
-11.0	–	–	–	–	–	AF Res.; [14], Cu(Zn)GeO_3: $J = J_{nn} + J_b$
-13.8	-4.9	–	–	0.36	–	HT Magn. Suscept. + magn.–stric.; [15]
-10.7	-3.7	–	–	0.35	–	HT Magn. Spec. Heat from Raman Scat.; [16]
-9.02	–	0.050	-0.50	–	–	Raman spectra: [17].

Table 3: The variation of the magnetic susceptibility with pressure from [22], the lattice constants with pressure from: [23]. In the final column we find the variation of the principle bond angle.

Direction i	$delta \ln \chi_i / \delta P_i$ [%/GPa]	c_{ii} [GPa]	$\delta \ln i / \delta P_i$ [% /GPa]	$\delta J_{nn} / \delta P_i$ [meV/GPa]
a	-2.5	66	-1.5	-0.60
b	+5	24	-4.2	+1.20
c	+1	300	-0.3	+0.24

Table 4: Parameter values used in the calculation of the superexchange interaction. Energies are in eV.

$t_{dp\sigma}$	1	U_d	7	U_{pxx}	5	$J_{pd\pi}$	0.025
$W_{pp\sigma}$	1	$J_{Hund,O}$	0.4	U_{pyy}	5	J_{dz^2,dx^2-y^2}	1
δ_{dp}	4.0	$J_{d\pi d\sigma}$	1	U_{pxy}	4.2	δ_p	0.4

Table 5: The exchange constants as calculated in the various perturbation approximations described in the text. We give only the parameters which differ from the ones given in table 4.

A: Perturbation results for the simple Ge–O hybridization model. The geometrical dependence of the two–site pd exchange is not explicit taken into account. Parameters: $t_{pd} = 0.9$; $\delta_\sigma = 4$; $J_{apd} = 0.017$; $J_{bpd} = 0.018$; $J_{cpd} = 0.029$.

B: Perturbation results for the simple Ge–O hybrization model for the Cu_2O_2 cluster. Parameters: $t_{pd} = 0.9$; $\delta_\sigma = 4$; $J_{p\sigma d\sigma} = 3J_{p\pi d\sigma}$; $J_{p\pi d\pi} = 0$; $J_{p\sigma d\pi} = 0.5J_{p\pi d\sigma}$.

C: Perturbation result for the $Cu_2O_2Ge_2$ cluster, the p_y–p_z mixing is neglected. Parameters: $\delta_\sigma = 4$; $J_{cpd} = 0.026$ (0.053); $J_{apd} = 0.031$;
$J_{bpd} = 0.032$; $J_{xpd} = 0.053$; $J_{ypd} = 0.045$.

Model	A	B	C	experiment
$J_{c,nn}$ 300 K	9.8	102	7.8	13.8 [15]
20 K	10.1	10.6	8.0	–
4 K (1)	10.8	11.2	9.2	–
(2)	9.0	9.6	6.4	–
$J_{c,nnn}$	3.2	3.2	5.2 (4.20)	4.9 [15]
$J_{a,nn}$	0.02	–	-0.03	-0.1[6]
$J_{a,nnn}$	-0.02	–	-0.07	–
$J_{b,nn}$	0.06	–	0.02	1.0 [6]
$J_{b,nnn}$	-0.02	–	-0.08	–
$\delta \ln J_{c,nn}/\delta\beta$	20 %	18 %	30–45 %	5.8 %
$\delta \ln J_{c,nn}/\delta\alpha$	0.5%	0.5 %	4.8 %	2.0 %
γ (20 K)	0.32	0.3	0.66(0.52)	0.36[15]

Table 6: The exchange constants for the exact solution of:

The Cu_2O_2 plaquette. Parameters used: $t_{pd} = 1.0$, $W = .9$; $\epsilon_{0d} = -4.0$; $U_d = 7$, $V_{0\sigma} = 3.7$; $\Delta_\sigma = 6.65$; $J_{pd} = 0.03$; $\epsilon_{0px} = -13.4$; $U_x = U_y = 5.0$; $U_{xy} = 3.8$.

Band model: Parameters used are the same as for the plaquette except: $\epsilon_{0d} = -3.7$; $J_{pd} = 0.04$; $J_{OH} = 0.6$. All energies are in eV. Exchange constants in meV. The structural parameters we used are those at 20 K.

Model	α	β	J_{nn}	γ	$\delta \ln J_{nn}/\delta\beta$	$\delta \ln J_{nn}/\delta\alpha$
Cu_2O_2 plaquette	158.85	9.24	13.5	–	9.7 %	0.56 %
band model	158.85	9.24	14	.31	10 %	1 %
experiment	–	–	13.8 [15]	0.36 [15]	5.8 %	2 %

Figure 1: The CuO_2 ribbon, with the Ge side groups, and the tetragonal distortion of the Cu coordination by O: the four O2 form a rectangular coordination of Cu, while the two O1 are shifted along the "tetragonal" axis rather far away from Cu. The bridge angle ϕ and hinge angle α are indicated.

Figure 2: The *nn* and *nnn* transfer paths for superexchange in the *b* direction. The *nn* exchange in the *b* direction is between Cu–0 and Cu–1, and the *nnn* exchange is between Cu–0 and Cu–1'. The bond lengths and angles used in the calculation are indicated. For details see the text.

Figure 3: The *nn* and *nnn* transfer paths for superexchange in the *a* direction. The *nn* exchange is between Cu–0 and Cu–1 is along two Cu–O–O–Cu transfer paths, while the *nnn* to Cu–1' is along one of these transfer path. The various bond lengths and angles used in the text are indicated.

Figure 4: The SP transition. We emphasize the SP distortion as predominantly one where the angles are changing. In the SP phase the dimerization of the Cu chain is predominantly due to the occurrence of two sets of angles (ϕ_1, α_1) and (ϕ_2, α_2), the bridge and hinge angle respectively.

Figure 5: The accordion effect due to pressure along the *b*–axis, viewed along the *c*–axis. The CuO_2 ribbon/chains as well as the GeO_3 chains are rotating with respect to each other as rigid units, around the shared O2 ions: the hinges. Thereby the hinge angle α decreases. In the figure we keep the GeO_3 chain in unit A fixed. Arrows indicate the movement of the neighbor units: CuO_2 ribbon, and the GeO_3 chains w.r.t. to this fixed unit. The direction and length of these arrows is only a general indication of the type of distortion.

Figure 6: A simplified representation of the distortion due to pressure along the *b*–axis. The hinges are at the O2 atoms. We emphasize the central role of the hinge angle in the distortion of the lattice: both Ge–O bonds move clock–wise, leaving the bond lengths constant; thereby the hinge angle α decreases.

Figure 7: Exchange along the c–axis. We have indicated the various transfer matrix elements used in the text: t_{pd} between Cu-d and O-p, $W_{\|}$ and $W_{\perp}$ – the pp transfer between two nn O along and perpendicular to the Cu chain, and $V_{0\sigma}$ – the σ–type transfer between the Ge-sp^3 hybrid and an O-p orbital. Also the energies of the local unperturbed states at the Cu (ϵ_{0d}) and on the O (ϵ_{0p}) are indicated. The nn superexchange is between Cu–0 and Cu–1, the nnn superexchange between Cu–0 and Cu–2.

Figure 8: The original quantization axes for 90^0 superexchange. The angle β is the deviation of the bridge angle M_1–L_i–M_2 (ϕ) from 90^0. The $d_{x'^2-y'^2}$ orbitals on the M_1 and M_2 and the $p_{x'}$ and $p_{y'}$ orbitals on the ligands L_1 and L_2 are shown. The transfer matrix elements between the ligand p and magnetic d orbital is t.

Figure 9: The new quantization axes. The axes x' and y' are rotated over 45^0 to x and y, with respect to those used in fig. 8. The σ–bonding orbitals on the side groups S_1 and S_2 are shown. The angle β is the deviation from ideal 90^0 geometry. The transfer integral between d_{xy} and p_x is t, and the transfer integral between the p_y orbitals on the two ligands L_1 and L_2 is W.

Figure 10: The Cu_2O_2GeSi cluster. We illustrate the local distortion due to Si substitution. The O which is bonded to the Si is shifted along the Si–O bond in the direction of Si. The bridge angle (ϕ) decreases while the hinge angle (α) increases.

Figure 11: Results of the band model: the nn superexchange (J_{nn}: full line) and the ratio of the nnn and nn superexchange (γ: dashed line) as a function of the deviation of the bridge angle $\beta = \phi - 90^0$. We used the following values for the parameters: Parameters used: $t_{pd} = 1.0$, $W = .9$, $\epsilon_{0d} = -3.4$, $U_d = 7$, $V_{0\sigma} = 3.7$, $\Delta_\sigma = 6.65$, $J_{pd} = 0.03$, $J_{OH} = 0.6$ All energies are in eV.

Figure 12: Results of the band model: the nn superexchange (J_{nn}: full line) and the ratio of the nnn and nn superexchange – the frustration parameter γ: dashed line – as a function of the hinge angle ϕ. The parameters used are the same as in fig. 11

Figure 13: Results of the band model: the nn superexchange J_{nn} (full line), the frustration parameter γ (dotted line) (ratio of the nnn and nn superexchange), the derivative of J_{nn} w.r.t. the bridge angle α (long dashes), and J_{nn} w.r.t the hinge angle β (short dashes) as a function of the Ge–O hybridization V_σ. The parameters used are the same as in fig.: 11

Figure 14: Results of the band model: the nn superexchange J_{nn} (full line), the frustration parameter γ (dotted line) (ratio of the nnn and nn superexchange), the derivative of J_{nn} w.r.t. the bridge angle α (long dashes), and J_{nn} w.r.t the hinge angle β (short dashes) as a function of the energy difference between the O-p and Ge-sp^3 hybrid: d_σ. The parameters used are the same as in fig. 11

$CuGeO_3$ c-axis

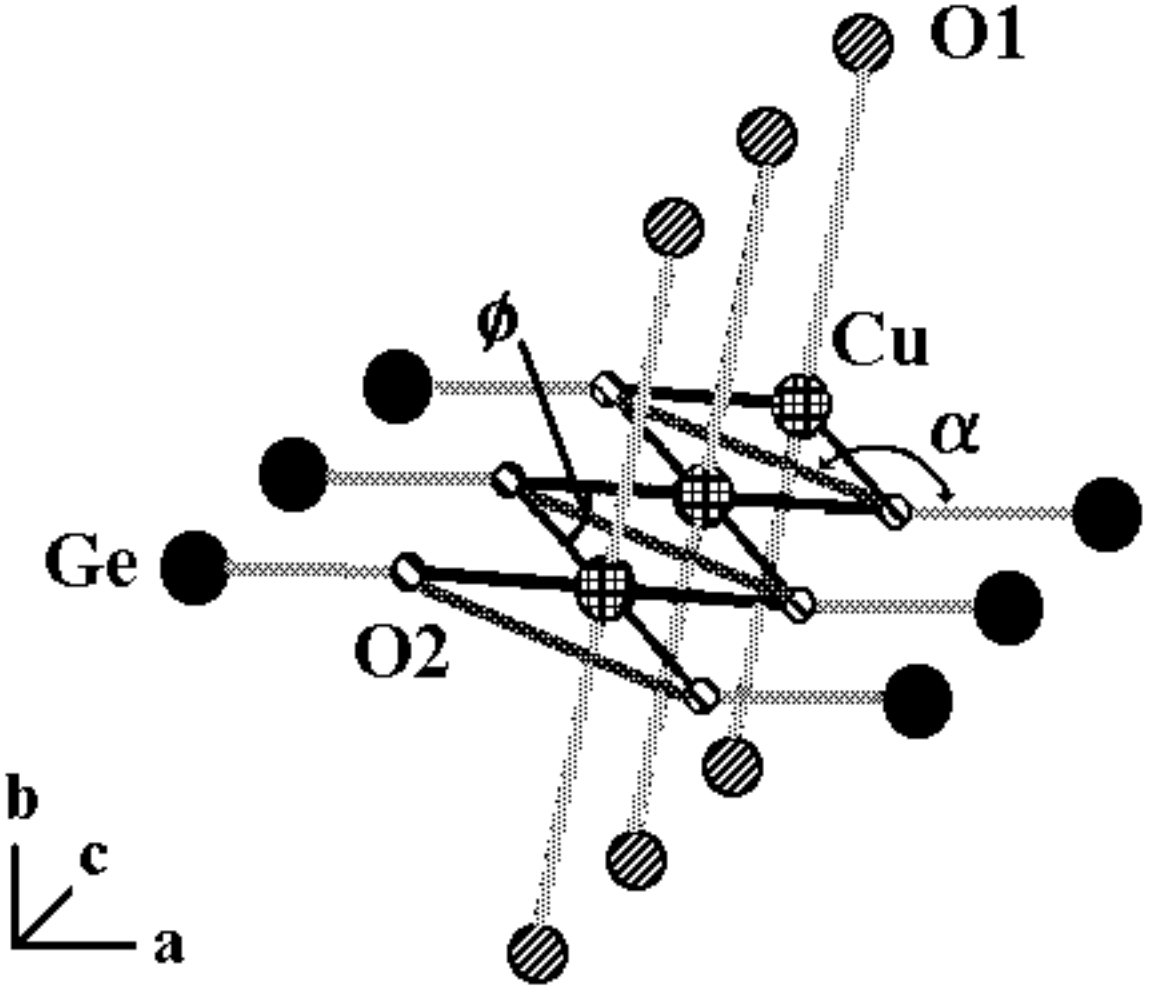

Geertsma
Khomskii

Fig. 1

$CuGeO_3$ J_{nn} : 01_b

b - axis J_{nnn}: $01'_b$

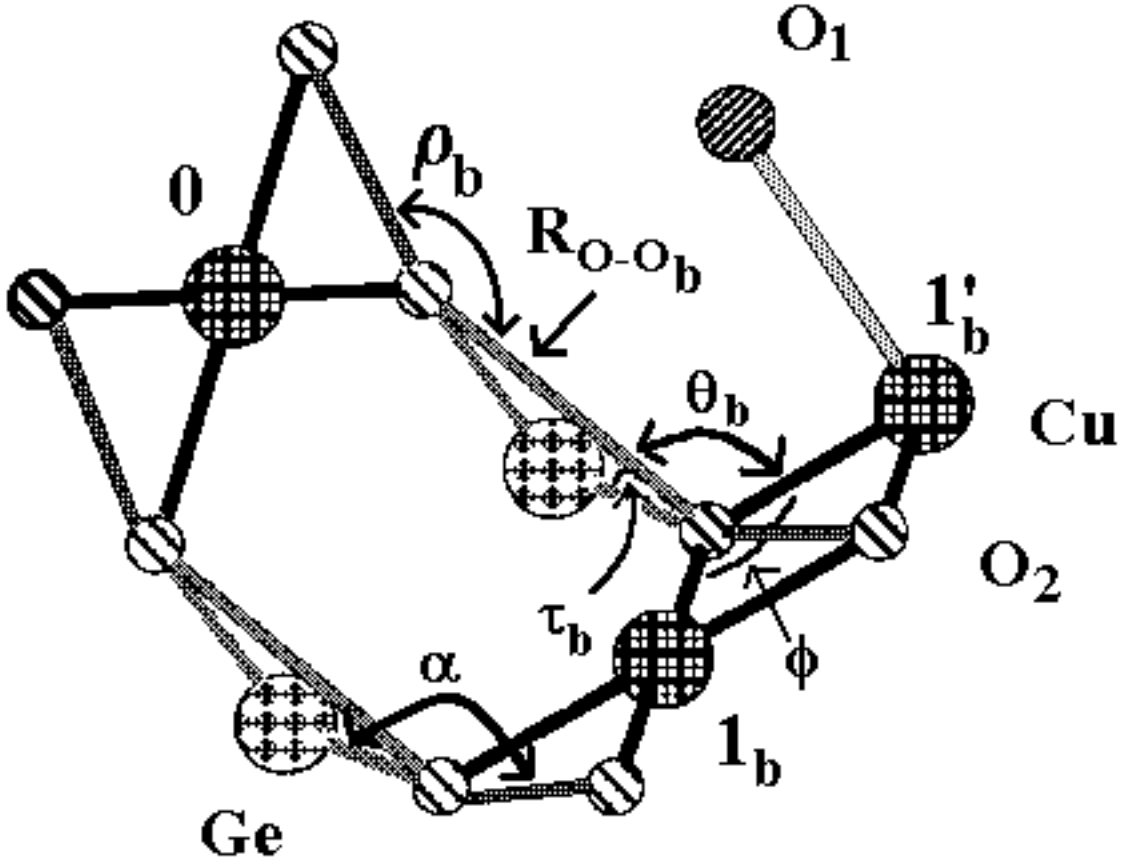

Geertsma
Khomskii

Fig. 2

$CuGeO_3$ J_{nn} : 0 1_a

a - axis J_{nnn}: 0 $1'_a$

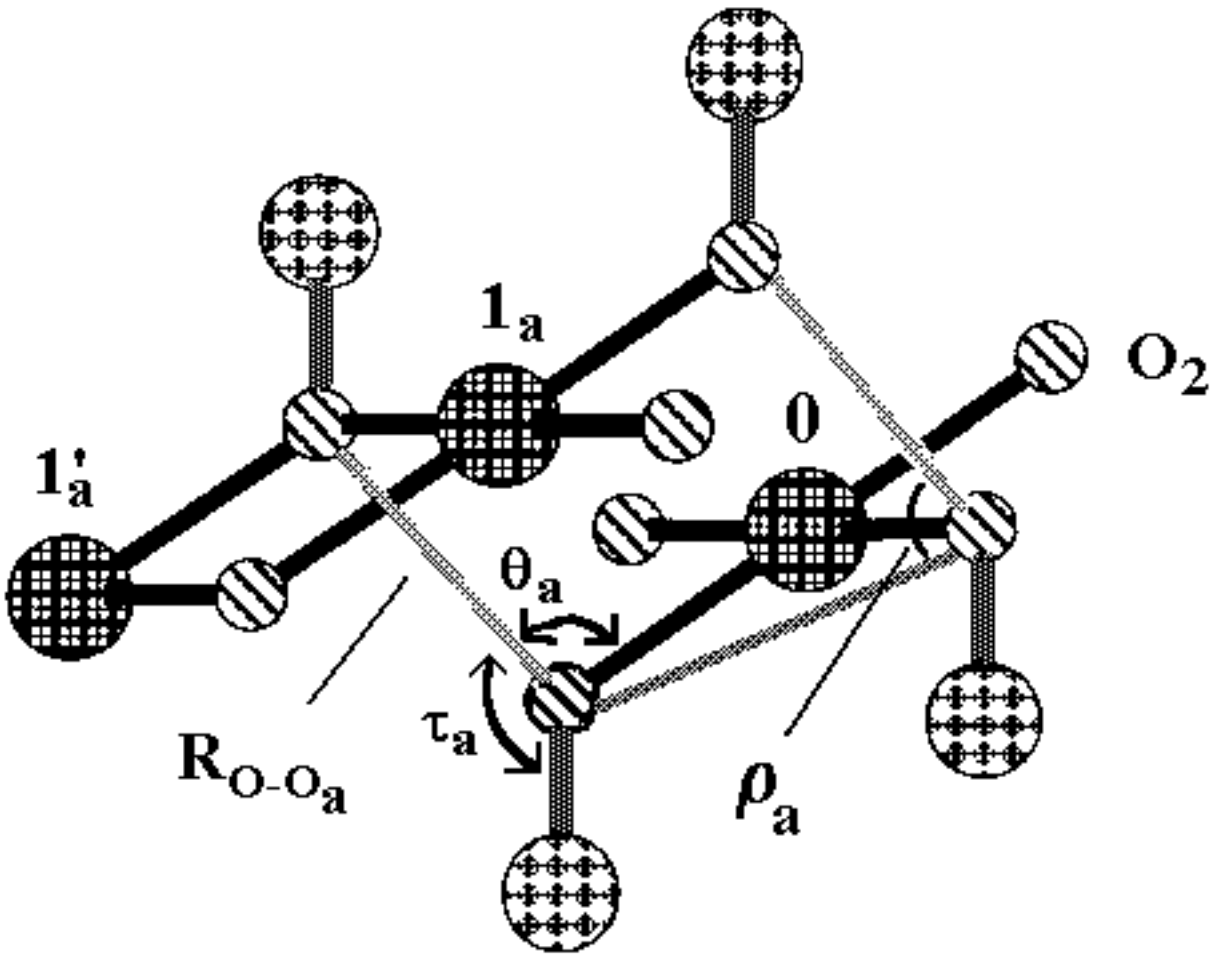

Geertsma
Khomskii

Fig. 3

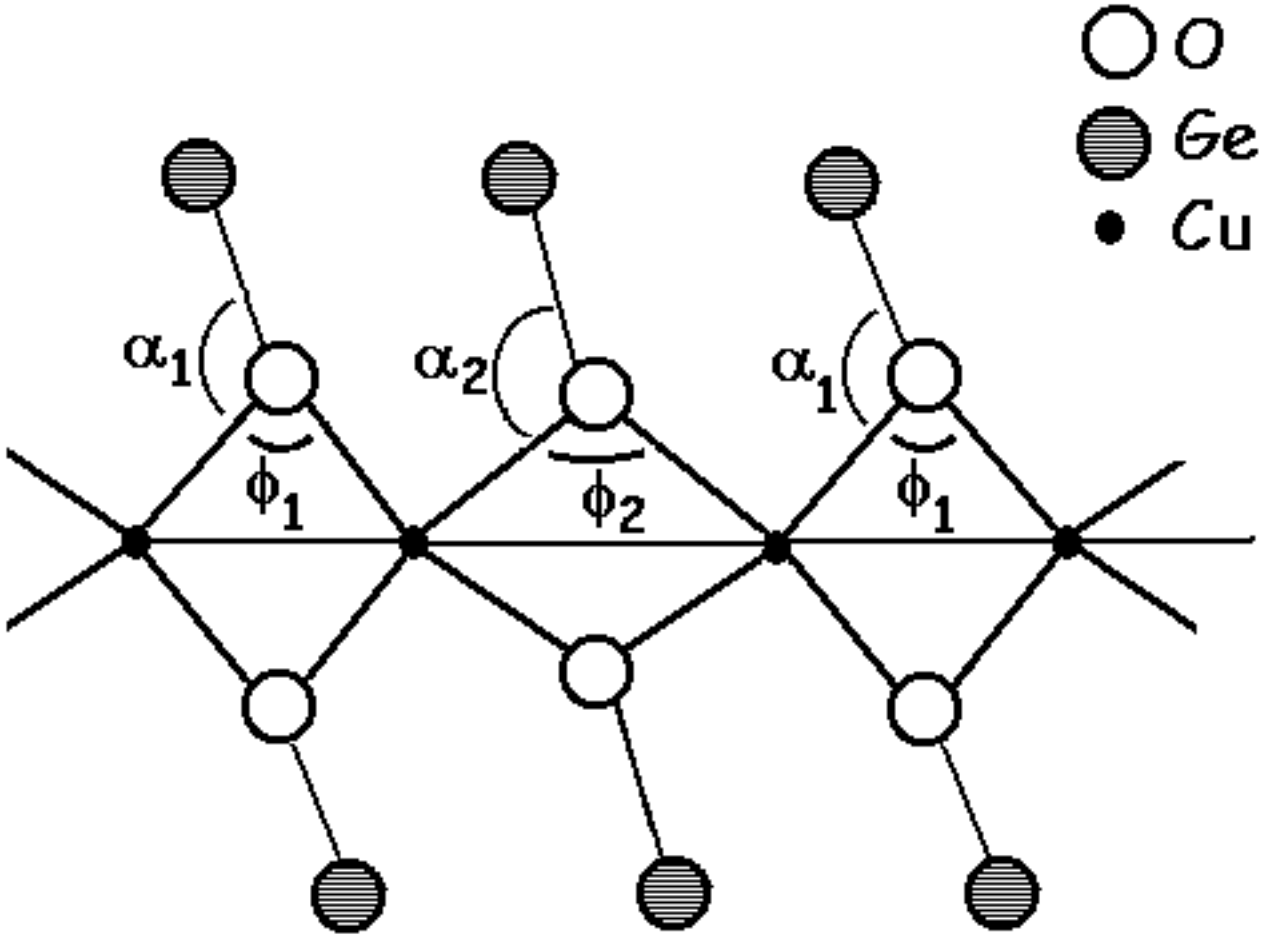

Geertsma
Khomskii

Fig. 4

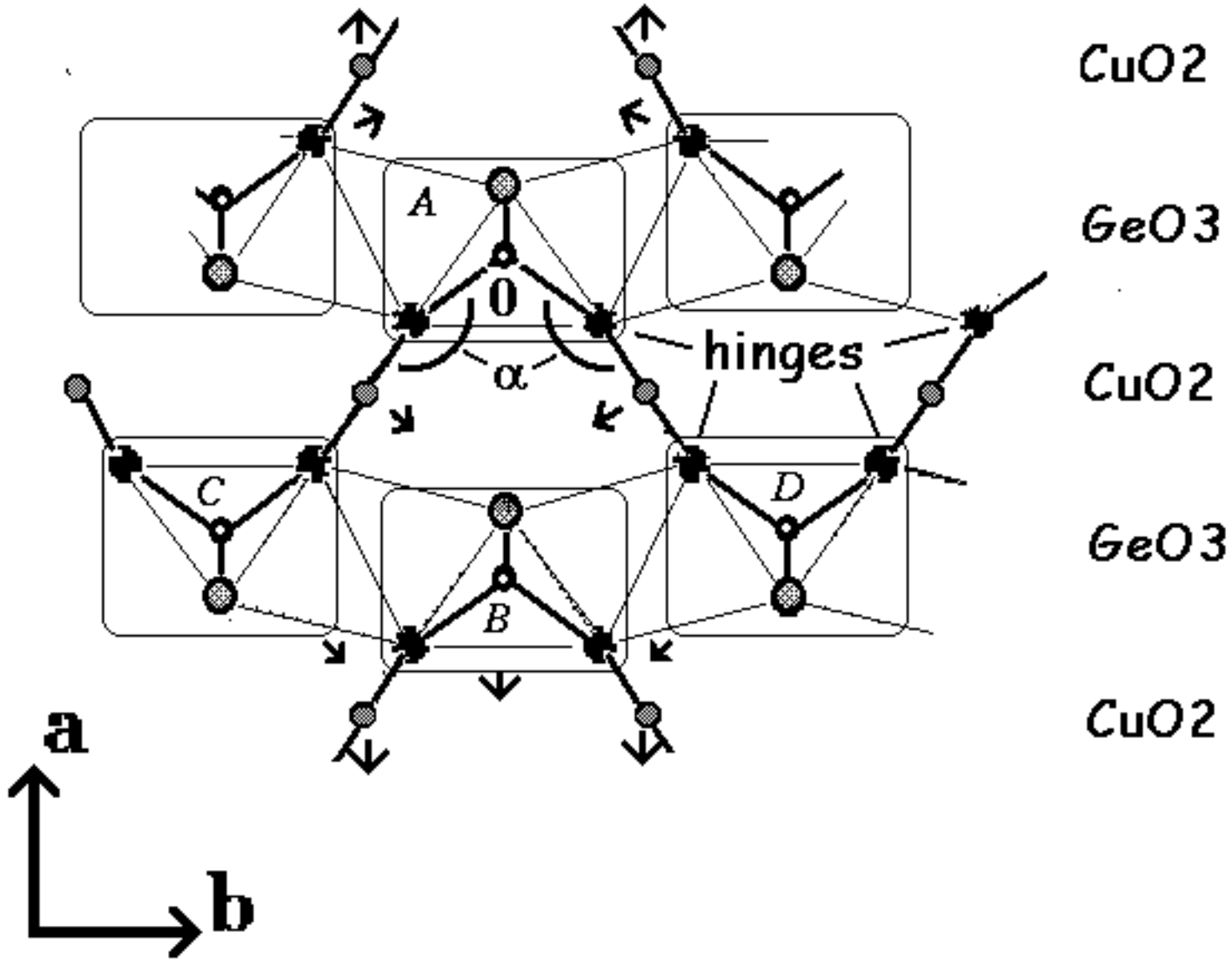

Geertsma
Khomskii

Fig. 5

$CuGeO_3$ J_{nn} : 01

c - axis J_{nnn}: 02

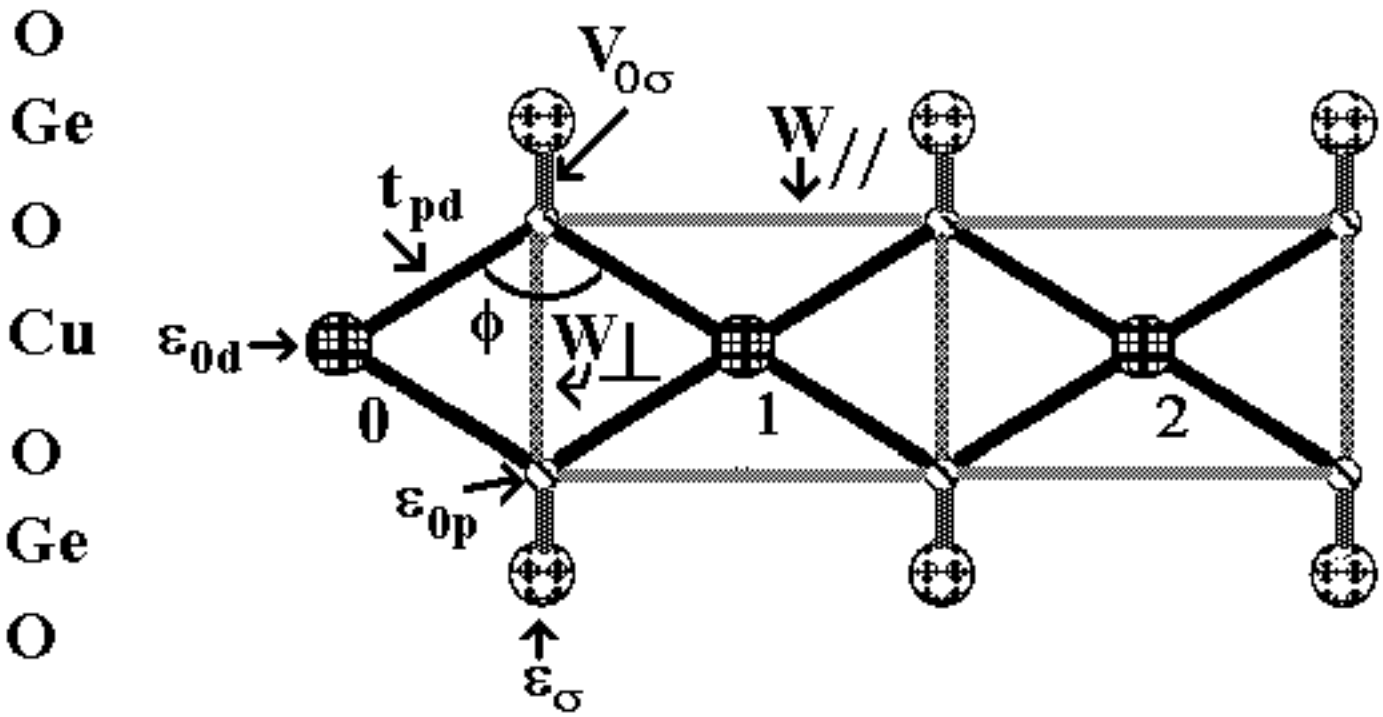

$\phi = \pi/2 + \beta$

Geertsma
Khomskii

Fig. 7

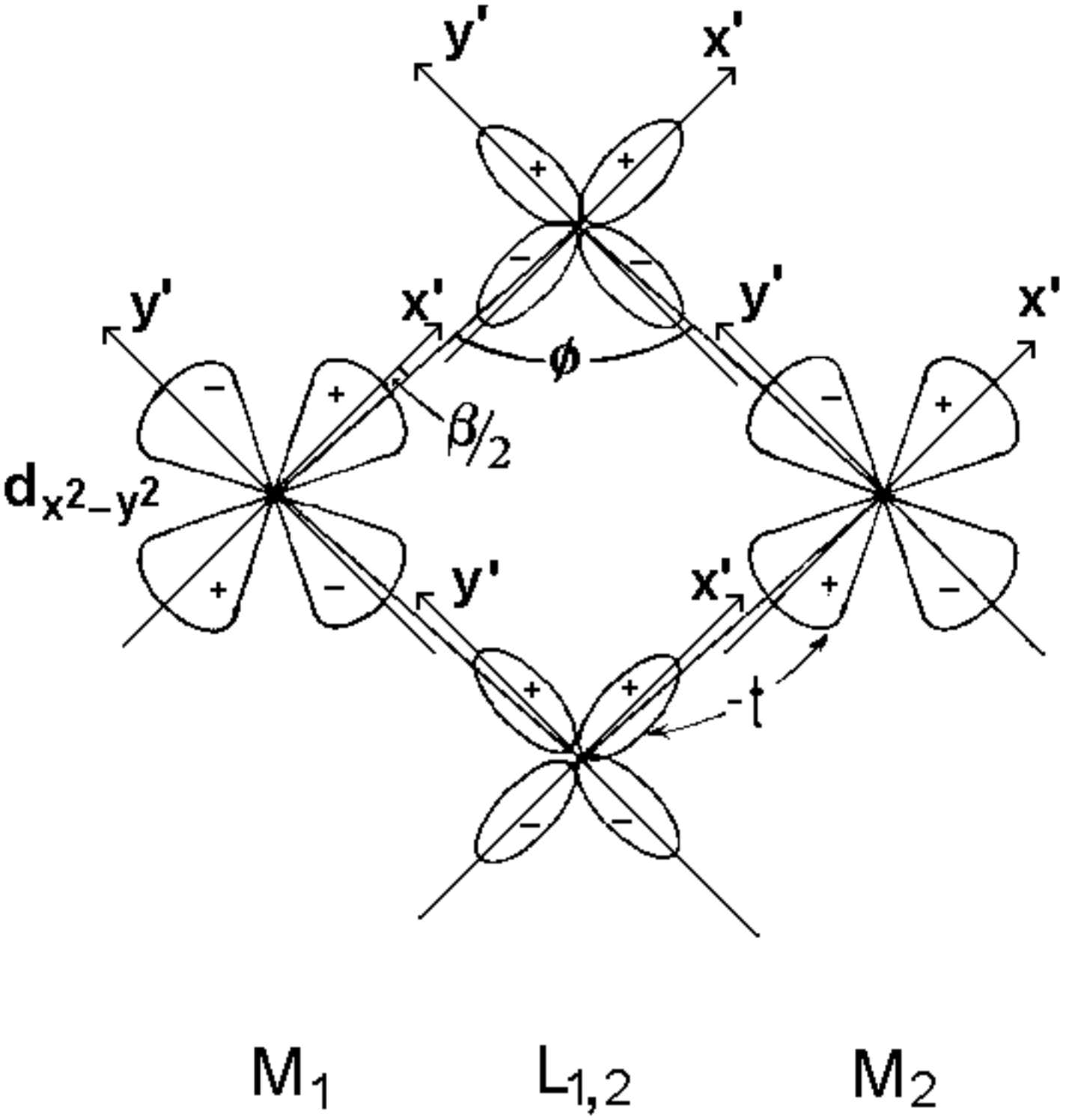

Geertsma
Khomskii

Fig. 8

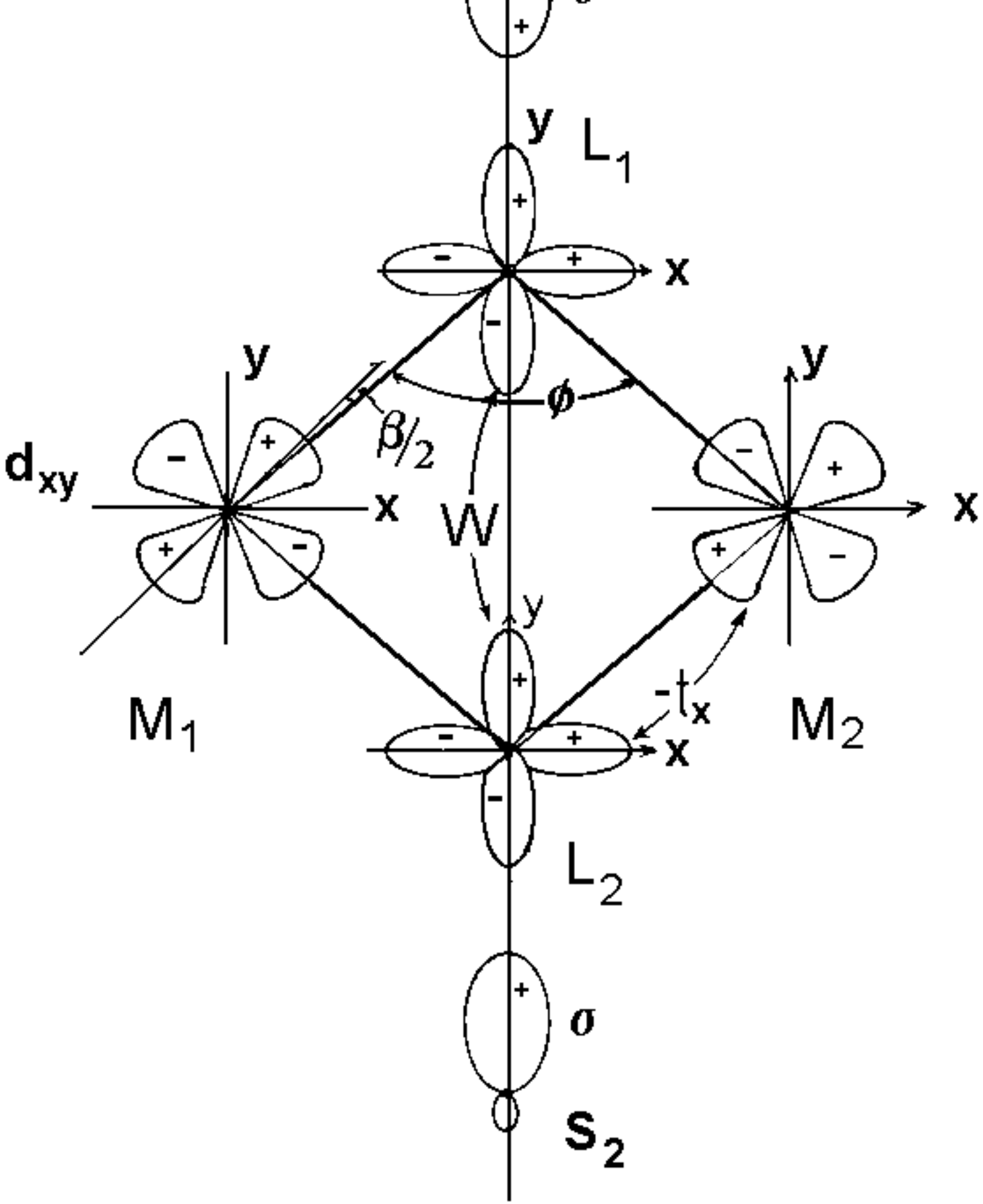

Geertsma
Khomskii

Fig. 9

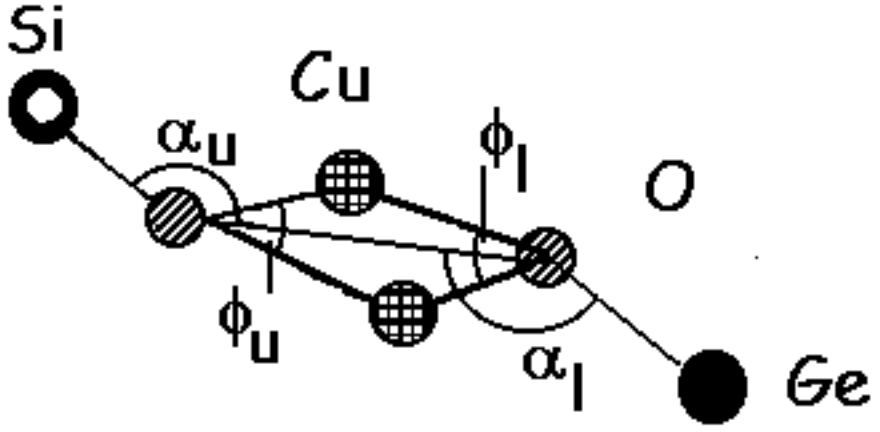

Geertsma
Khomskii

Fig. 10

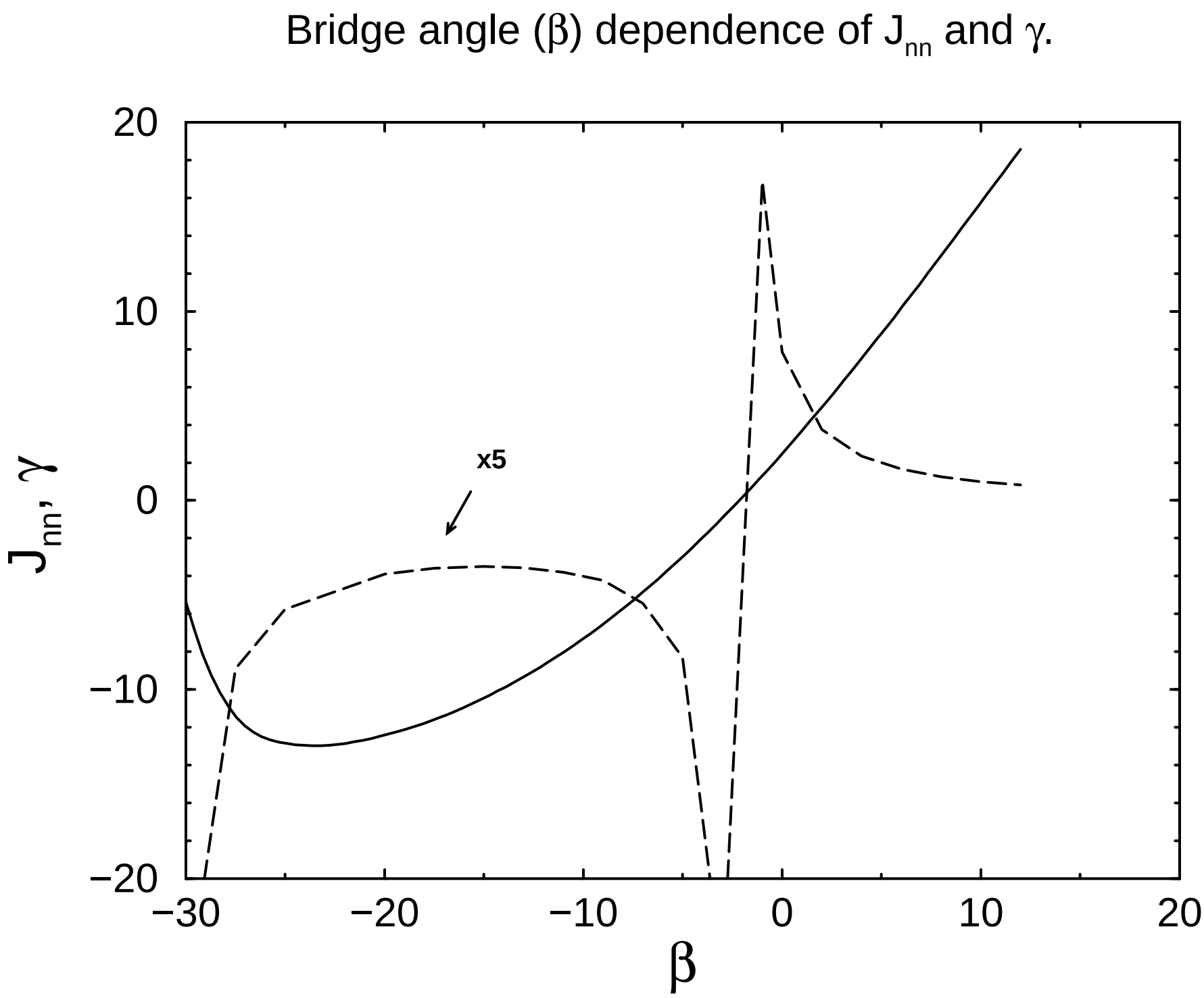
Bridge angle (β) dependence of J_nn and γ.
20
10
0
−10
−20
−30
−20
−10
0
10
20
β
J_nn, γ
x5

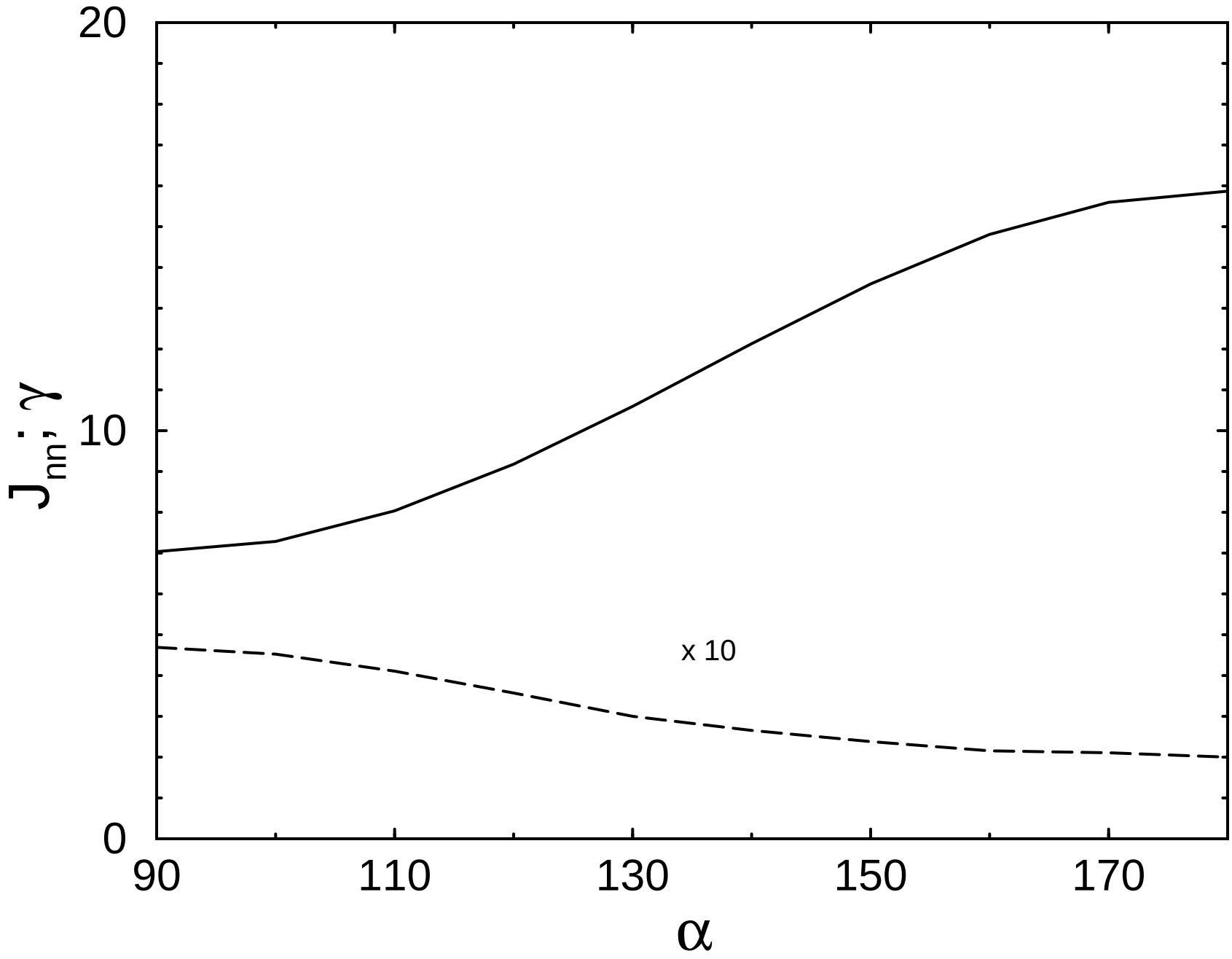
Hinge Angle (α) dependence of J_nn and γ = J_nnn/J_nn
20
10
0
J_nn ; γ
x 10
90
110
130
150
170
α

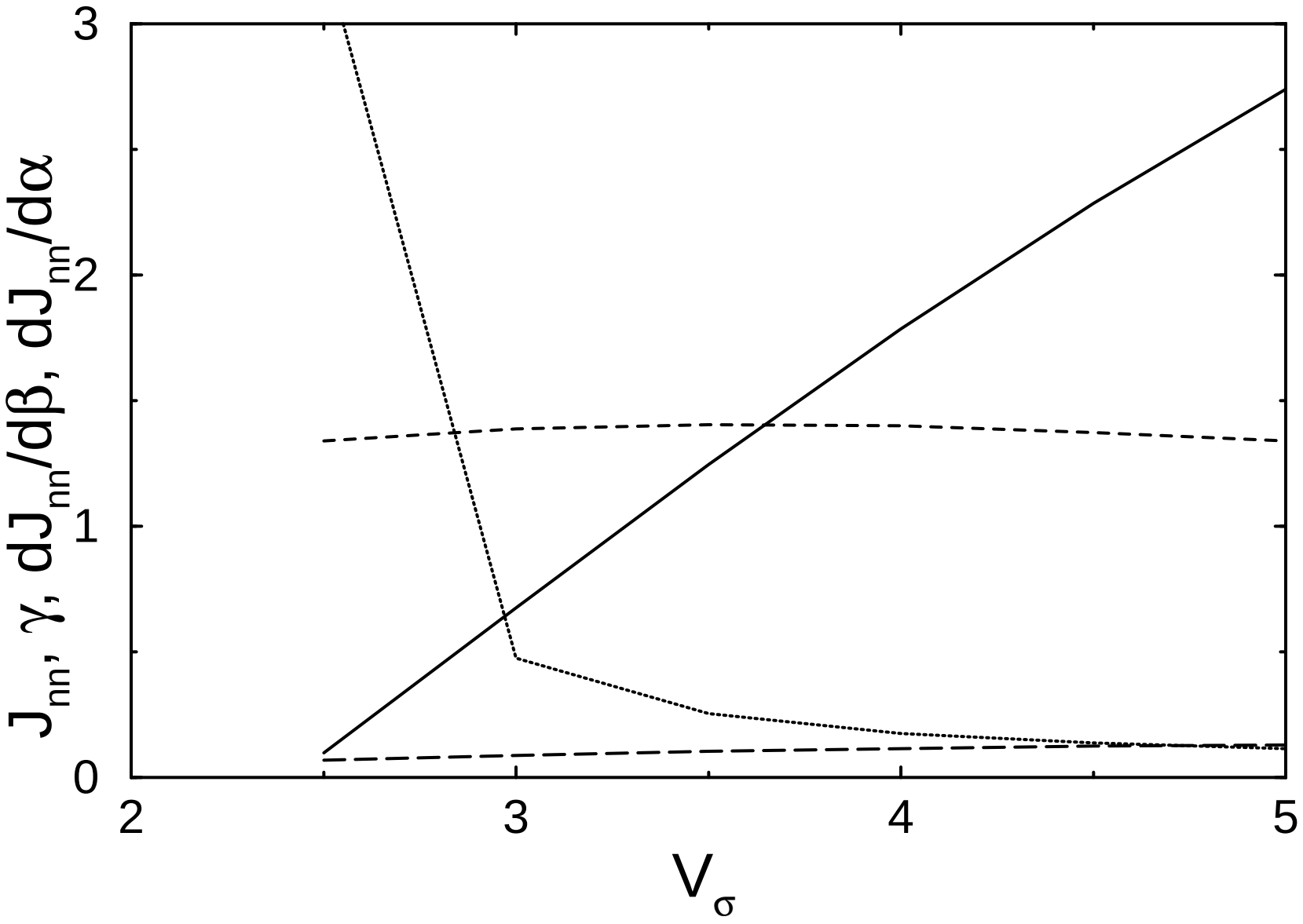
Chemical variations: V_σ
J_{nn}, γ, $dJ_{nn}/d\beta$, $dJ_{nn}/d\alpha$
V_σ
0
1
2
3
2
3
4
5

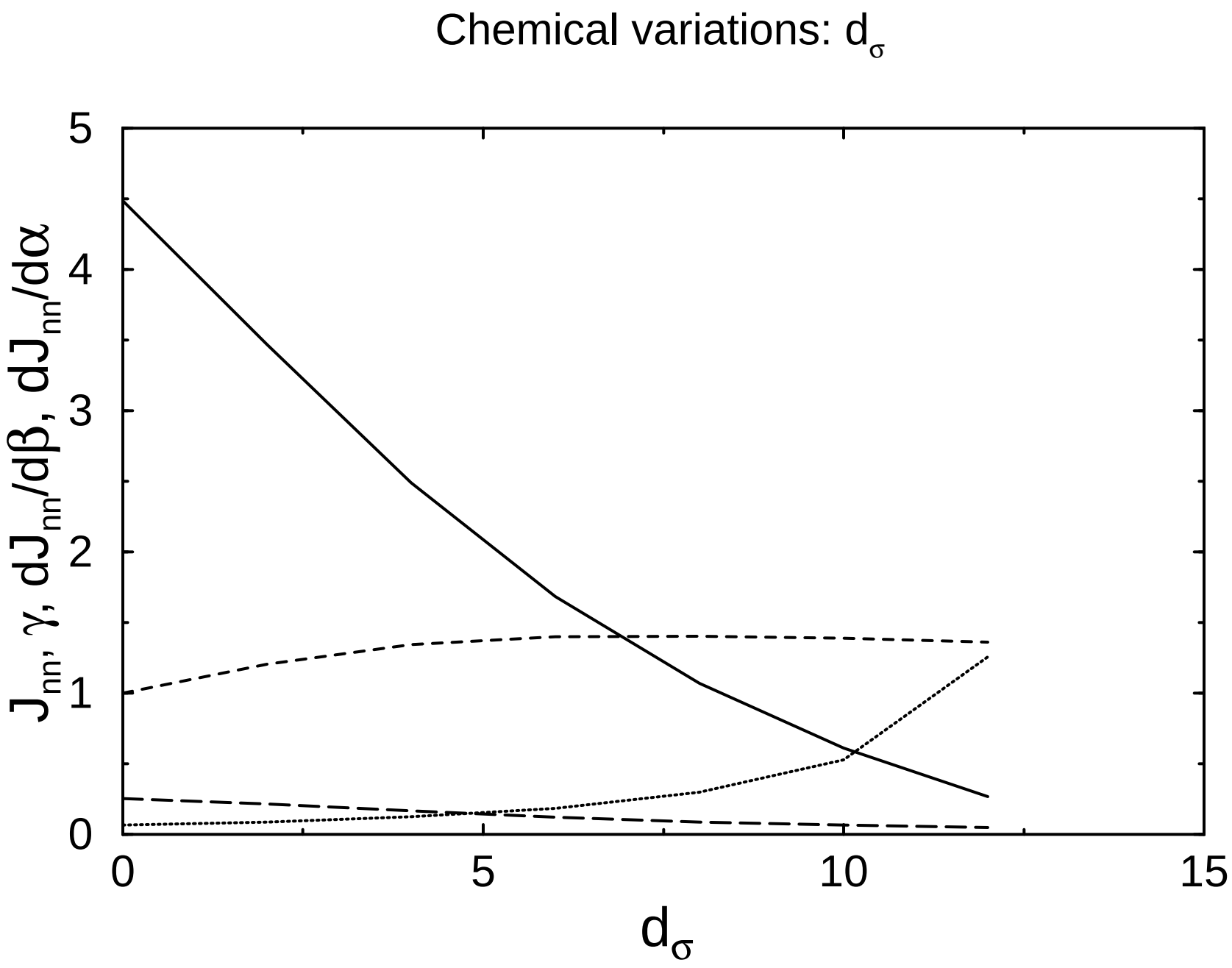
Chemical variations: d_σ
J_{nn}, γ, $dJ_{nn}/d\beta$, $dJ_{nn}/d\alpha$
0
1
2
3
4
5
0
5
10
15
d_σ